

CrystEngComm

Accepted Manuscript



This is an *Accepted Manuscript*, which has been through the Royal Society of Chemistry peer review process and has been accepted for publication.

Accepted Manuscripts are published online shortly after acceptance, before technical editing, formatting and proof reading. Using this free service, authors can make their results available to the community, in citable form, before we publish the edited article. We will replace this *Accepted Manuscript* with the edited and formatted *Advance Article* as soon as it is available.

You can find more information about *Accepted Manuscripts* in the [Information for Authors](#).

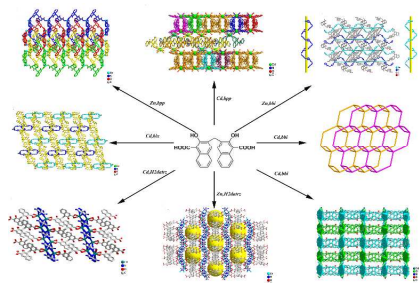
Please note that technical editing may introduce minor changes to the text and/or graphics, which may alter content. The journal's standard [Terms & Conditions](#) and the [Ethical guidelines](#) still apply. In no event shall the Royal Society of Chemistry be held responsible for any errors or omissions in this *Accepted Manuscript* or any consequences arising from the use of any information it contains.

Assembly of a series of d^{10} Coordination Polymers of Pamoic Acid through Mixed-Ligand Synthetic Strategy:

Syntheses, Structures and Fluorescent Properties

Tingting Cao^a, Yanqiang Peng^{a,c}, Suna Wang^{a,*}, Jianmin Dou^a, Yunwu Li^a, Jing Lu^a, Ting Liu^a, Dacheng Li^a, Junfeng Bai^{b,*}

Eight fluorescent coordination compounds were obtained based on H₂PA and N-donor ligands through mixed-ligand synthetic strategy.



Cite this: DOI: 10.1039/c0xx00000x

www.rsc.org/xxxxxx

ARTICLE TYPE

Assembly of a series of d¹⁰ Coordination Polymers of Pamoic Acid through Mixed-Ligand Synthetic Strategy: Syntheses, Structures and Fluorescent Properties

Tingting Cao,^a Yanqiang Peng,^a Ting Liu,^a Suna Wang,^{*a} Jianmin Dou,^a Yunwu Li,^a Changhui Zhou,^a Dacheng Li,^a and Junfeng Bai^{*b}

Received (in XXX, XXX) Xth XXXXXXXXX 20XX, Accepted Xth XXXXXXXXX 20XX

DOI: 10.1039/b000000x

Eight mixed-ligand coordination compounds, [Zn(PA)(bpp)]_n (**1**), {[Cd(PA)₂(Hbpp)₂(H₂O)₂]·2H₂O}_n (**2**), [Zn(PA)(bbi)]_n (**3**), [Cd(PA)(bbi)(H₂O)]_n (**4**), {[Cd₃(PA)₂(bbi)₃(Cl)₂]}_n (**5**), 10 {[Zn₆(PA)₅(datrz)₂(Hdatrz)₂(H₂O)₂]·16DMF}_n (**6**), [Cd₂(PA)(datrz)₂(DMF)₂]_n (**7**), and 15 {[Cd₂(PA)₂(bix)₂(DMF)₂]·4DMF}_n (**8**) (bpp = 1,3-bis(4-pyridyl)propane, bbi = 1,4-bis(imidazol-1-yl)butane, H₂datrz = 3,5-diamino-1,2,4-triazole, bix = 1,4-bis(imidazol-1-ylmethyl)benzene) have been synthesized through the reaction of zinc and cadmium salts with pamoic acid (H₂PA) and different N-donor ligands. The assembly of the ligands in different coordination modes and conformations lead to 15 fascinating structures. **1** and **3** afford interpenetrating polythreaded 2D→3D motif composed of 4⁴ sql undulated sheets, while right- and left-helices are alternatively arranged in **3**. **2** possesses an interesting 3-D supramolecular network with 1-D hydrogen-bonded chains spanning in different directions. **4** and **5** displays both polyrotaxane and polycatenane characteristics. In **4**, two 2,4-connected (4.8⁵) nets interlocked with each other, forming a 2D→2D polycatenating network. **5** exhibits a two-fold 20 interpenetrated (3,5,6)-connected (3.5.6)(3.5².6⁷)(3².5⁴.6⁶.7².9) topology. **6** and **7** represent rare pentanodal (3,4)-connected and bimodal (3,4)-connected frameworks with the topology of (4.5.6)(4.8.10)(5².6.8.9.11)(4.5.6.8.9²)(4.5.7) and (4.6.8)(4.6².8³), respectively. **8** displays 3-fold interpenetrated 4-connected SrAl₂ topology with flexible bix ligands bridging Cd centers to form right- and left-helices. The mixed-ligand effect of the conformations of PA ligand and N-heterocyclic coligands 25 as well as the metal centers on the assembly of frameworks is unravelled in details. Solid-state luminescent properties of all compounds were reported as well. Moreover, fluorescent properties of compounds **6** and **8** in various solvent suspensions at room temperature have been also investigated.

Introduction

During the past decades, interest has grown tremendously in the design and construction of novel functional coordination polymers (CPs) or metal-organic frameworks (MOFs) for fascinating structures and elegant topologies as well as potential applications in luminescence, magnetism, separation, catalysis, nonlinear optics, and gas storage.¹⁻⁴ Based on empirical

observation and understanding of the construction of building blocks, a certain degree of structural design and prediction of these polymers can be achieved, which was known as rational design strategy.⁵⁻⁶ The prediction and design of exact structures, however, is still a great challenge considering the complicated factors that could have influences on the resulting networks, such as coordination geometry of metal ions, structural characteristics of ligands, solvent system, counter anions, and so on.

As important building units, ligands with specific symmetry and rigidity/flexibility are crucial to control and adjust the architectures of CPs or MOFs. Mixed-ligand synthetic strategy, which combines the advantages of different types of ligands, can be rationally proposed.⁷⁻⁹ When different ligand components are allowed to combine with the metal ions, each ligand will not only compete to interact with the metal centers but also cooperate with each other by adjusting their conformations to generate coordination diversity of the metal centers and further the geometry of the metal nodes. As a consequence, more meaningful architectures with novel properties may be resulted compared

^a Shandong Provincial Key Laboratory of Chemical Energy Storage and Novel Cell Technology, School of Chemistry and Chemical Engineering, Liaocheng University, Liaocheng, P. R. China. Tel: +86-0635-8230669; ^b State Key Laboratory of Coordination Chemistry, School of Chemistry and Chemical Engineering, Nanjing National Laboratory of Microstructures, Nanjing University, Nanjing, P. R. China Tel: +86-025-83593384; Email: wangsun@lcu.edu.cn; bjunfeng@nju.edu.cn.

† Electronic Supplementary Information (ESI) available: cifs of the compounds, syntheses of the compounds, additional figures, photoluminescence and TG of the compounds. See DOI: 10.1039/b000000x/

with those structures based on single kind of ligands. The typical and reliable research now was mainly focused on the polycarboxylate and N-containing ligands. As acid and basic ligands, these two kinds of ligands are perfect partners considering charge balance, coordination deficiency, repulsive vacuum, and weak interactions. For a given polycarboxyl ligand, for example, different variety of N-donor ligands may construct a wide range of desired coordination networks. Exploration of the essential factors in such structural assembly may provide further insights in designing new hybrid crystalline materials.

Previously, we have constructed a series of intriguing CPs assembled from flexible polycarboxyl ligands with different exo-bidentate N-containing auxiliary ligands.¹⁰ Existence of $-CH_2-$ groups in these aromatic carboxylate ligands makes them possess both rigid and flexible characters, which can adopt various conformations via bending, stretching, or twisting depending on the coordination requirement of the metal center and the competition and cooperation of different N-coligands. In this work, we reported eight mixed-ligand CPs obtained from reactions of Zn and Cd salts and pamoic acid (H_2PA , 4,4'-methylenebis(3-hydroxy-2-naphthylcarboxylic acid)) in the presence of N-donor ligands with different flexibility and symmetry. Eight compounds, namely, $[Zn(PA)(bpp)]_n$ (**1**), $[Cd(PA)_2(Hbpp)_2(H_2O)_2] \cdot 2H_2O$ (**2**), $[Zn(PA)(bbi)]_n$ (**3**), $[Cd(PA)(bbi)(H_2O)]_n$ (**4**), $\{[Cd_3(PA)_2(bbi)_3(Cl)_2]\}_n$ (**5**), $\{[Zn_6(PA)_5(datrz)_2(Hdatrz)_2(H_2O)_2] \cdot 16DMF\}_n$ (**6**), $[Cd_2(PA)(datrz)_2(DMF)_2]_n$ (**7**), and $\{[Cd_2(PA)_2(bix)_2(DMF)_2] \cdot 4DMF\}_n$ (**8**) ($bpp = 1,3$ -bi(4-pyridyl)propane, $bbi = 1,4$ -bis(imidazol-1-yl)butane, $H_2datrz = 3,5$ -diamino-1,2,4-triazole, $bix = 1,4$ -bis(imidazol-1-ylmethyl)benzene) were fully characterized by X-ray single crystal diffraction, IR, TG, and XRD. The effects of the conformations of PA ligand, the introduction of different N-heterocyclic coligands as well as the coordination geometry of the metal ions on the assembly of frameworks are unravelled in details. Fluorescence properties of all compounds and of compounds **6** and **8** in different solvent suspensions have also been performed.

Experimental

Materials and general methods

Pamoic acid was purchased from Alfa-aesar. 3,5-diamino-1,2,4-triazole (H_2datrz) and 1,3-bi(4-pyridyl)propane (bpp) were purchased from Sigma-Aldrich. 1,4-bis(imidazol-1-ylmethyl)benzene (bix) and 1,4-bis(imidazol-1-yl)butane (bbi) were synthesized according to previous literatures.¹¹ Other reagents were commercially available and used as purchased without further purification. The hydrothermal reactions were carried out in 23 mL stainless steel autoclaves lined with Teflon under autogenous pressure. The emission/excitation spectra were recorded on a Hitachi 850 fluorescence spectrophotometer. C, H and N analyses were carried out with a Perkin-Elmer 240C elemental analyzer. The FT-IR spectra (4000-400 cm^{-1} region) were recorded from KBr pellets with a VECTOR 22 spectrometer. Powder X-ray diffraction (PXRD) data were collected over the 2θ range 5-50° on a Philips X'pert diffractometer working with $Cu K\alpha$ radiation ($\lambda = 1.5418 \text{ \AA}$) at room temperature.

Thermogravimetric analyses were performed under nitrogen with a heating rate of 10°C/min on a TGA V5.1A Dupont 2100 instrument from room temperature to 700 °C.

Synthesis of $[Zn(PA)(bpp)]_n$ (**1**)

A mixture of H_2PA (38.8 mg, 0.1 mmol), $Zn(NO_3)_2 \cdot 6H_2O$ (29.6 mg, 0.10 mmol) and bpp (19.8 mg, 0.1 mmol) in DMF/ H_2O ($v/v=1/2$, 12 mL) was placed in a Parr Teflon-lined stainless steel vessel (23mL) and heated to 120°C for 48h. Then the reaction system was cooled to room temperature slowly and colorless block crystals of **1** were obtained. After filtration, the crystals were washed with water and dried in air. Yield: 36.9% (based on H_2PA and $Zn(NO_3)_2 \cdot 6H_2O$). $C_{36}H_{28}N_{20}O_6Zn$ ($Mr = 649.99$): calcd. C 66.52, H 4.34, N 4.31; found C 66.42, H 4.35, N 4.41. IR (KBr pellet): 3435(vs,br), 2937(w), 1645(m), 1620(s), 1558(m), 1508(w), 1453(s), 1386(s), 1330(s), 1246(w), 1206(w), 1070(w), 819(w), 735(w), 600(w), 559(w) cm^{-1} .

Synthesis of $[Cd(HPA)_2(bpp)_2(H_2O)_2] \cdot 2H_2O$ (**2**)

The procedure was the same as that of **1** except that $Zn(NO_3)_2 \cdot 6H_2O$ was replaced by $Cd(NO_3)_2 \cdot 4H_2O$ (30.8 mg, 0.10 mmol). Yield: 39.5% (based on H_2PA and $Cd(NO_3)_2 \cdot 4H_2O$). $C_{72}H_{70}N_{40}O_{18}Cd$ ($Mr = 1391.73$): calcd. C 62.14, H 5.07, N 4.03; found C 62.08, H 4.99, N 4.06. IR (KBr pellet): 3433(vs,br), 2925(w), 1639(m), 1614(m), 1557(m), 1395(m), 1090(w), 810(w), 751(w) cm^{-1} .

Synthesis of $[Zn(PA)(bbi)]_n$ (**3**)

The procedure was the same as that of **1** except that bpp was replaced by bbi (19.0 mg, 0.1 mmol). Yield: 41.9% (based on H_2PA and $Zn(NO_3)_2 \cdot 6H_2O$). $C_{33}H_{28}N_{40}O_6Zn$ ($Mr = 641.98$): calcd. C 61.74, H 4.40, N 8.73; found C 61.78, H 4.45, N 8.76. IR (KBr pellet): 3441(s,br), 2924(m), 1644(m), 1559(w), 1455(w), 1386(m), 1112(w), 952(w), 833(w), 737(w) cm^{-1} .

Synthesis of $[Cd(PA)(bbi)(H_2O)]_n$ (**4**)

The procedure was the same as that of **3** except that $Zn(NO_3)_2 \cdot 6H_2O$ was replaced by $Cd(NO_3)_2 \cdot 4H_2O$ (30.8 mg, 0.10 mmol). Yield: 35.5% (based on H_2PA and $Cd(NO_3)_2 \cdot 4H_2O$). $C_{33}H_{30}N_{40}O_7Cd$ ($Mr = 707.02$): calcd. C 56.06, H 4.28, N 7.92; found C 56.01, H 4.25, N 7.96. IR (KBr pellet): 3423(vs,br), 1647(s), 1588(m), 1537(m), 1499(m), 1452(m), 1409(s), 1300(w), 1105(w), 856(w), 777(m), 721(w) cm^{-1} .

Synthesis of $\{[Cd_3(PA)_2(bbi)_3(Cl)_2]\}_n$ (**5**)

The procedure was the same as that of **4** except that $Cd(NO_3)_2 \cdot 6H_2O$ was replaced by $CdCl_2$ (18.3 mg, 0.10 mmol). Yield: 32.7% (based on H_2PA and $CdCl_2$). $C_{76}H_{70}N_{12}O_{12}Cl_2Cd_3$ ($Mr = 1751.57$): calcd. C 52.11, H 4.03, N 9.60; found C 52.60, H 3.98, N 9.72. IR (KBr pellet): 3445(vs,br), 2929(w), 1646(s), 1559(m), 1509(m), 1458(s), 1394(s), 1357(m), 1232(w), 1090(w), 760(m), 656(w) cm^{-1} .

Synthesis of $\{[Zn_6(PA)_5(datrz)_2(Hdatrz)_2(H_2O)_2] \cdot 16DMF\}_n$ (**6**)

The procedure was the same as that of **1** except that bpp was replaced by H_2datrz (9.9 mg, 0.1 mmol). The reaction was performed at 80°C for 48h. Then the reaction system was cooled to room temperature slowly and colorless block crystals of **6** were obtained. After filtration, the crystals were washed with water

and dried in air. Yield: 33.6% (based on H₂PA and Zn(NO₃)₂·6H₂O). C₁₇₁H₂₀₄N₃₆O₄₈Zn₆ (3924.12): calcd. C 52.34, H 5.24, N 12.85; found C 52.60, H 5.28, N 13.08. IR (KBr pellet): 3428(vs,br), 1657(s), 1641(s), 1552(w), 1510(w), 1452(m), 1390(m), 1234(w), 810(w), 759(w) cm⁻¹.

Synthesis of {[Cd₂(PA)(datrz)₂(DMF)₂]_n (7)

The procedure was the same as that of **6** except that Zn(NO₃)₂·6H₂O was replaced by Cd(NO₃)₂·4H₂O (30.8 mg, 0.10 mmol). Yield: 42.5% (based on H₂PA and Cd(NO₃)₂·4H₂O). C₃₃H₃₆N₁₂O₈Cd₂ (953.56): calcd. C 41.57, H 3.81, N 17.63; found C 41.60, H 3.85, N 17.66. IR (KBr pellet): 3437(vs,br), 2359(w), 1652(s), 1572(w), 1518(m), 1450(m), 1391(s), 1237(w), 1101(w), 813(w), 764(w) cm⁻¹.

Synthesis of {[Cd₂(PA)₂(bix)₂(DMF)₂·4DMF]_n (8)

The layered diffusion method was employed at room temperature. A solution of bix (27.6 mg, 0.15 mmol) in CH₃OH (3 mL) was carefully layered on a solution of Cd(NO₃)₂·4H₂O (30.8 mg, 0.10 mmol) and H₂PA (38.8 mg, 0.10 mmol) in DMF (3 mL). Colorless single crystals of **8** were obtained in a few days. Yield: 42.9% (based on H₂PA and Cd(NO₃)₂·4H₂O). C₉₅H₁₀₅N₁₅O₁₉Cd₂ (1985.76): calcd. C 57.46, H 5.32, N 10.58; found C 57.75, H 5.26, N 10.62. IR (KBr pellet): 3435(vs,br), 2924(w), 1640(s), 1510(w), 1459(m), 1397(m), 1103(w), 812(w), 551(m) cm⁻¹.

X-ray Crystallography

Suitable single crystals of compound **5** and **6** were measured on Agilent at 110 and 104 K, respectively. Crystals of other compounds were selected for indexing and intensity data were measured on a Siemens Smart CCD diffractometer with graphite-monochromated Mo K α radiation ($\lambda = 0.71073\text{\AA}$) at 298 K. The raw data frames were intergrated into SHELX-format reflection files and corrected using SAINT program. Absorption corrections based on multi-scan were obtained by the SADABS program. The structures were solved with direct methods and refined with full-matrix least-squares technique using the SHELXS-97 and SHELXL-97 programs, respectively.¹² Displacement parameters were refined anisotropically, and the positions of the H-atoms were generated geometrically, assigned isotropic thermal parameters, and allowed to ride on their parent carbon atoms before the final cycle of refinement. Basic information pertaining to crystal parameters and structure refinement is summarized in Table 1, and selected bond lengths and angles are listed in Table S1. All the structures were examined using the Addsym subroutine of PLATON to ensure that no additional symmetry could be applied to the models. Selected bond lengths and angles are given in Table S1. CCDC 1004651-1004657 and 1004650, contain the supplementary crystallographic data for this paper. Topological analysis of coordination networks in all compounds was performed with the program package TOPOS. In compounds **6** and **8**, the solvent molecules are highly disordered, and attempts to locate and refine them were unsuccessful. The SQUEEZE program was used to remove scattering from the highly disordered solvent molecules.¹³ The structure was solved by using the new generated .HKL file. The solvent molecules were assigned according to EA and TG data.

In compound **1**, C atoms (C33/C33', C34/C34') of bpp ligand

are disordered over two general positions with a site occupancy of 0.516(13)/0.484(13), respectively. In compound **2**, C atoms (C30/C30', C31/C31') of bpp ligand are disordered over two general positions and refined isotropically with a site occupancy of 0.49(3)/0.51(3). In compound **5**, C atoms (C38/C38', C39/C39') of bbi ligand are disordered over two general positions and refined isotropically with a site occupancy of 0.726(11)/0.274(11). In compound **6**, Zn3 centers were disordered and refined isotropically with a site occupancy of 0.626(8)/0.374(8). In compound **7**, C atoms (C15/C15', C16/C16') of DMF molecule were refined isotropically with a site occupancy of 0.46(4)/0.54(4).

Results and discussion.

Syntheses of the compounds.

Four kind of N-coligands (bpp, bbi, datrz and 1,4-bix) with different characters were employed in this study in order to explore the effect of the introduction of auxiliary ligands on the formation of unique frameworks. The resulting products were largely different for different systems. The assembly of the frameworks was susceptible to the species of the metal ions, the N-heterocyclic coligands and the conformations of PA ligand as well as reaction conditions. Reactions with the same starting materials were carried out through both solvothermal and layer diffusion methods, while only the syntheses reported here generated suitable single crystals for X-ray diffraction. Except for compound **8** which was formed by layer diffusion method, other compounds were all obtained in solvothermal conditions. Recently, we have reported several MOFs based on PA ligands using both methods, especially three supramolecular isomeric compounds.^{10a, 14} Formation of the products is largely dependent upon the conditions, especially the temperature, which could control the kinetical or thermodynamical conformers to some extent.

Structural descriptions.

{[Zn(PA)(bpp)]_n (1)

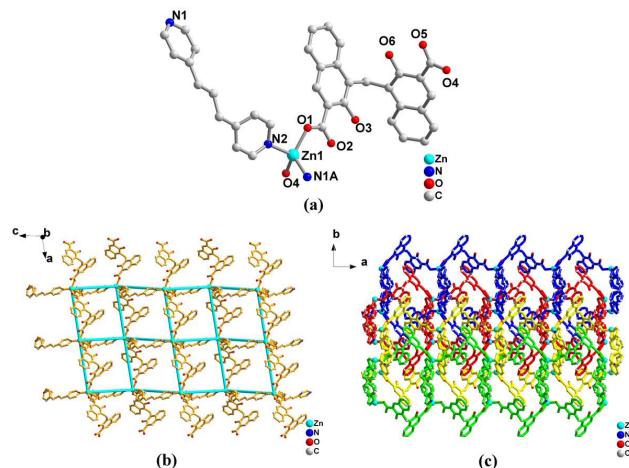


Figure 1. (a) The coordination environment of Zn atom in **1**. Symmetry code: A, -x, +y, 3/2-z. (b) Perspective of the 2-D corrugated layer, showing the 4-connected sql net. (c) Perspective view of the 2D→3D polythreading framework of **1** along the c axis.

Single-crystal X-ray diffraction analysis indicates that compound **1** crystallizes in the monoclinic system and $P2_1/c$ space group. As depicted in Figure 1a, the asymmetric unit is composed of one Zn atom, one PA ligand and one bpp moiety. The tetrahedral coordination geometry around the metal center is completed by two monodentate carboxylate oxygen atoms (O1 and O4B) from PA ligands and two nitrogen atoms (N1A and N2) from bpp ligands. The Zn–O and Zn–N distances are in the range of 1.919(2)–2.034(3) Å. The PA ligand with bidentate $(\kappa^1)-(\kappa^1)-\mu_2$ coordination mode and bpp ligand in *TT* conformation act as linkers, connect Zn centers to form 2-D corrugated layers along the *ac* plane (Figure 1b). The dihedral angle of two pyridine rings of bpp is 132.5°. The Zn···Zn distances separated by PA and bpp ligands are 11.85(1) and 13.61(4) Å, respectively. PA ligand in this case adopts *cis* conformation and the dihedral angle between two naphthyl rings is 102.7°. Topologically, the layer could be represented by 4⁴ **sql** topology with Zn center as a slightly distorted 4-connected tetrahedral node.

Due to the big window and large corrugation of the layer, naphthyl rings of PA ligands in one layer can be threaded into the windows of two adjacent layers (Figure 1c and 1d). Consequently, the whole structure can be regarded as a 2D→3D polythreading framework.

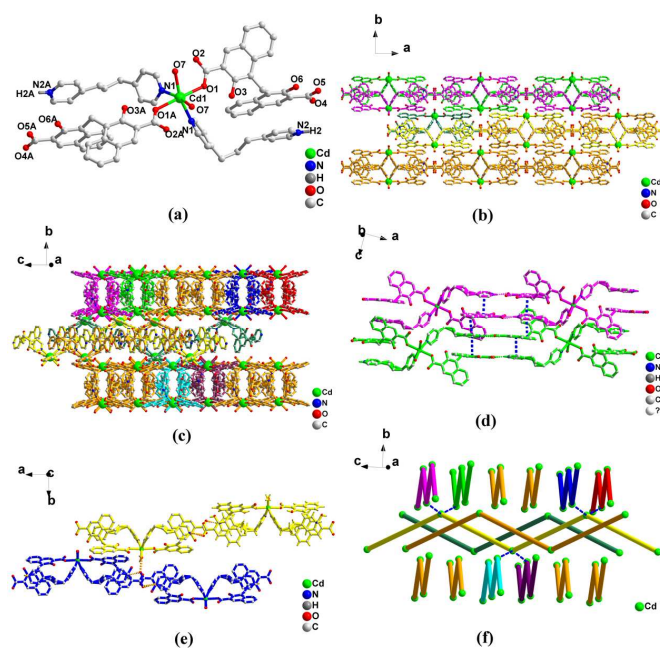
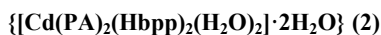


Figure 2. (a) View of the single molecule structure of **2**. Symmetry code: A, -x, +y, 3/2-z. (b) and (c) Perspective view of the 3-D supramolecular structure of **2** along the *c* and *a* axis, respectively. (d) and (e) Perspective view of the weak interactions between adjacent chains. (f) Topological representation of the 3-D supramolecular structure, showing each chain is connected with other six chains.

When Cd takes place of Zn, an interesting 3-D supramolecular structure based on a mononuclear molecule of compound **2** is

formed. **2** crystallized in orthorhombic crystal system and *Pbcn* space group. As illustrated in Figure 2a, in each molecule, Cd1 is surrounded by two monodentate carboxylate oxygen atoms (O1 and O1A) of two PA ligands, two nitrogen atoms (N1 and N1A) of monoprotonated bpp ligands and two aqua oxygen atoms (O7 and O7A), generating a six-coordinated CdN_2O_4 environment with slightly distorted octahedral geometry. The Cd–O and Cd–N distances are in the range of 2.314(4)–2.347(6) Å. Within the molecule, $\pi \cdots \pi$ stacking interactions are observed between the naphthyl rings of PA and pyridyl rings of bpp ligands with the centroid···centroid distance of 3.690 Å. The two carboxylate groups of PA ligand in this case adopt *cis* conformation and the dihedral angle between both naphthyl rings is 72.7°.

A more careful examination of the arrangement of the single molecules leads to exceptional finding (Figure 2b and 2c). The uncoordinated nitrogen atom (N2) of bpp ligand is protonated, which could form strong N–H···O interactions with the carboxylate oxygen atom (O4), linking adjacent molecules to form 1D zigzag chains along the *a* axis. The dihedral angle of two pyridine rings of bpp is 68.7°. The $\pi \cdots \pi$ stacking interactions are observed between the naphthyl rings of PA and pyridyl rings of bpp ligands from neighboring chains with the centroid···centroid distance of 3.732 Å (Figure 2d). Based upon these interactions, two identical sets of 2-D layers (A and B) are formed along the *ac* plane. Interestingly, the chains in A and B are not parallelly arranged but span two different stacking directions, respectively. To the best of our knowledge, the chains in 1-D structures are easily packed with a parallel orientation in one layer and less commonly span different directions.¹⁵ The O–H···O interactions existing between the aqua oxygen atom (O7) and carboxylate oxygen atom (O4) connect these layers further, resulting the overall 3-D supramolecular network (Figure 2e). Consequently, each chain interacts with eight neighboring chains within and between the layers through the two kinds of weak interactions (Figure 2f).



Compound **3** crystallizes in monoclinic crystal system and space group $P2_1/n$. As shown in Figure 3a, the asymmetric unit consists of one Zn center, one PA and one bbi ligands. Zn adopts 4-connected tetrahedral coordination geometry with two monodentate carboxylate oxygen atoms (O1 and O4A) from discrete PA ligands and two nitrogen atoms (N1 and N4B) from bbi ligands. The Zn–O and Zn–N distances are in the range of 1.929(3)–1.976(5) Å. The whole structure is also a (4,4) network with the window size of 11.5460(11)×9.5886(12) Å based on the Zn···Zn distances connected by PA and bbi ligands, respectively. Connectivity of the ligands and metal centers are more complicated than that of compound **1**. As shown in Figure 3b, bbi ligands adopt *GTT* conformation, linking Zn(II) centers to form helical chains. The repeated unit of Zn–bbi–Zn–bbi is along *b* axis with a pitch of 16.65(2) Å. The dihedral angle between two terminal imidazole rings is 78.8°. The two carboxylate groups of PA ligand adopt *cis* conformation and the whole ligand also acts as bidentate $(\kappa^1)-(\kappa^1)-\mu_2$ bridges to connect these helical chains. The dihedral angle between both naphthyl rings is 84.8°. As a result, a conjugated layer structure along the *ab* plane was obtained. The PA and bbi ligands are located at the lateral and

inside positions of the layers, respectively. The left- and right-handed Zn-bbi chains are arranged alternatively, leading to the overall nonchirality of the layer. Adjacent PA ligands exhibit interesting mirror-related conformations (Figure S1 in Supporting Information).

Due to large corrugation of the layer, naphthyl rings of PA ligands in one layer can be threaded into the windows of two adjacent layers through $\pi\cdots\pi$ stacking interactions with the aromatic rings. The centroid \cdots centroid distance between adjacent naphthyl rings of different layers is of 3.860 Å. As a result, the whole structures can be regarded as a 2D \rightarrow 3D polythreading motif involving three adjacent layers simultaneously (Figure 3c). The neighboring helical chains in different layers also exhibit opposite chirality.

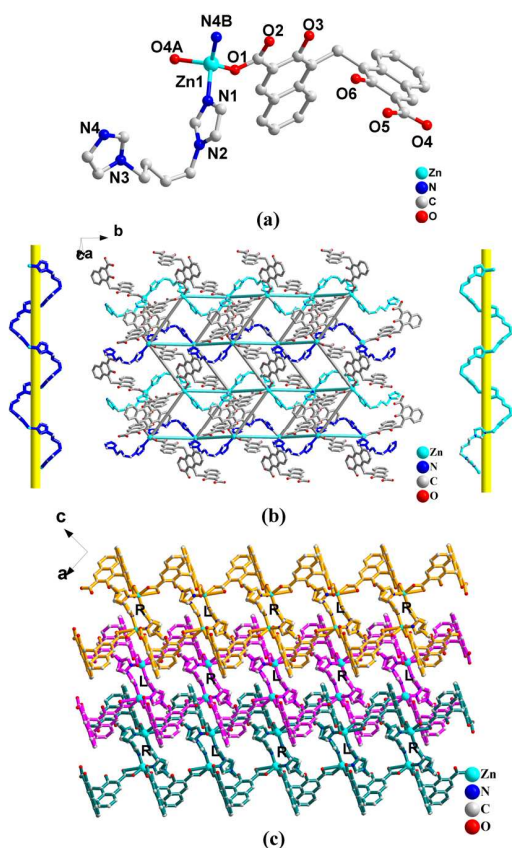


Figure 3. (a) View of the coordinated environment of Zn centers in **3**. Hydrogen atoms have been omitted for clarity. Symmetry codes: A, $-1/2+x, 1/2-y, -1/2+z$; B, $1/2-x, -1/2+y, -1/2-z$. (b) Perspective view of a single 2-D layer, showing the alternating helical Zn-bbi chains. Left and right-handed chains are represented in skyblue and blue, respectively. (c) Perspective view of 2D \rightarrow 3D polythreading motif of **3**.

25 $\{[\text{Cd}(\text{PA})(\text{bbi})(\text{H}_2\text{O})]_n\}$ (**4**)

Compound **4** crystallized in the space group $P2_1/n$ and presents uncommon interpenetrating network with both polyrotaxane and polycatenane motifs. The asymmetric unit has one Cd atom, one PA ligand and two half of bbi ligand (Figure 4a). Cd1 is coordinated with one monodentate carboxylate oxygen atom (O1), two bidentate carboxylate oxygen atoms (O4A and O5A), one

aqua oxygen atom (O7), as well as two nitrogen atoms (N1 and N3) of two half bbi ligands. The whole geometry is best described as a distorted octahedron. The Cd–O and Cd–N distances are in the range of 2.235(5)–2.437(5) Å. The PA ligand exhibits $(\kappa^1)-(\kappa^1-\kappa^1)-\mu_2$ coordination mode with two naphthyl planes in an approximately vertical arrangement with a dihedral angle of 76.8°.

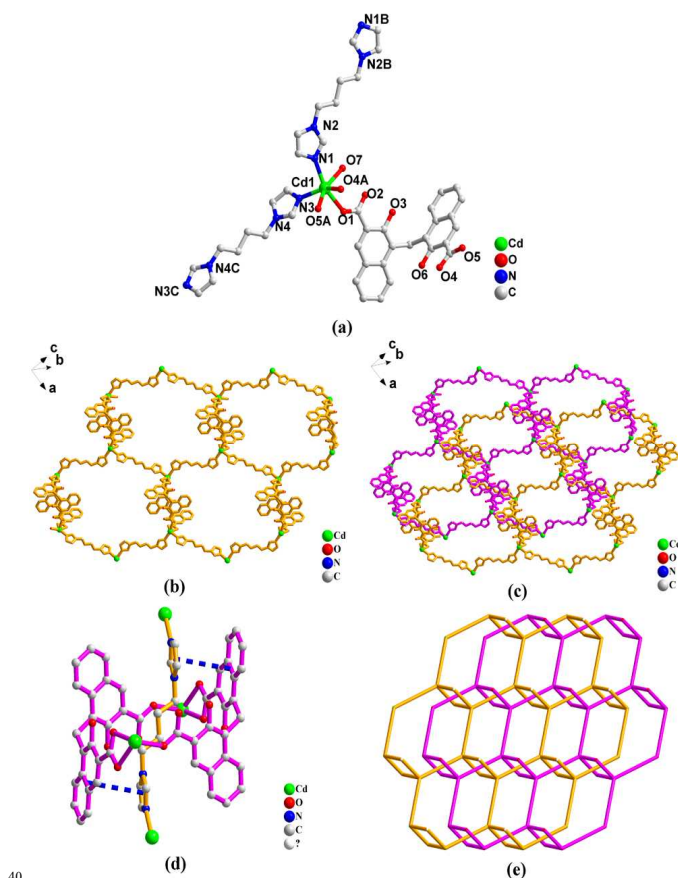


Figure 4. (a) The coordination environment around Cd center in **4**. Symmetry code: A, $2-x, -y, 2-z$; B, $1-x, 1-y, 3-z$; C, $-x, -y, 2-z$. (b) and (c) Perspective view of the 2-D net and 2-fold interpenetration of these nets. (d) Perspective view of the interactions of interlocked motifs. (e) Schematic description of such uncommon interlocked nets, showing the 2D \rightarrow 2D parallel polycatenation and polyrotaxane.

Two Cd centers are connected by two PA ligands, generating the Cd₂(PA)₂ loop. These loops are further linked by bbi ligands, forming 2-D sheet along the ac plane (Figure 4b). From a topological view, the sheet could be described as (4,4) topology with each Cd center acting as a node and two PA ligands simultaneously connecting two Cd centers as one linker. Two such nets in the structure, however, interlock with each other with the loops of each net penetrated by one bbi ligand of the other and vice versa, resulting 2D \rightarrow 2D polycatenating structure of the whole net (Figure 4c). The $\pi\cdots\pi$ stacking interactions are present between the interlocked loops with the centroid \cdots centroid distance between adjacent naphthyl ring and imidazole ring of 3.780 Å (Figure 4d). As a result, the fascinating structure possesses both polyrotaxane and polycatenane. Adjacent 2D

layers are arranged in AB mode, stacking to form a 3-D
supramolecular structure (Figure S2 in Supporting Information).
Consequently, if the loops are taken into account the whole net
could be better considered as 2,4-connected (4.8⁵) topology based
upon PA ligand and each metal center (Figure 4e). Previously,
Zheng *et al* have reported a similar metal-organic framework,
[Cd₂(bbi)(PA)₂], which was obtained from different synthetic
conditions and also possessed both polyrotaxane and
polycatenane characters, while the loop Cd₄(PA)₂ is composed
of four Cd atoms and two PA ligands.¹⁶

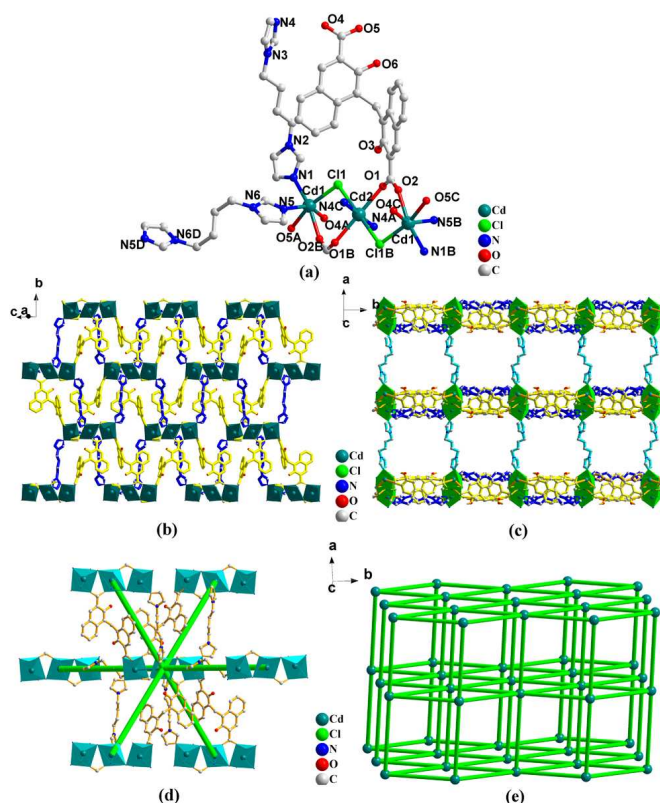


Figure 5. (a) The coordination environment around Cd center and the connectivity of trinuclear Cd₃ core in **5**. Symmetry codes: A, 1/2-x, 1/2+y, 1/2-z; B, 1-x, 1-y, 1-z; C, 1/2+x, 1/2-y, 1/2+z; D, 2-x, 1-y, -z. (b) and (c) Perspective view of the 2-D double-layer and 3-D pillared framework of **5** along bc plane and a axis, respectively. (d) The connectivity of each Cd₃ core with other six ones. (e) Topological representation of 6-connected net based on the Cd₃ cores.

Compound **5** crystallizes in the crystal system of monoclinic and space group *P2₁/c*. The asymmetric unit consists of one and a
half crystallographically independent Cd atoms, one PA ligand,
one (N3-N6, bbi1) and a half (N1-N2, bbi2) bbi ligands and one
Cl⁻ anion (Figure 5a). Cd centers are all in six-coordinated
distorted octahedral geometry. Cd1 is coordinated with two
carboxylate oxygen atoms (O2B and O5A) from two distinct PA
ligands, one nitrogen atom (N1) of bbi ligands, and Cl1 atom in
the equatorial plane. One bbi nitrogen atom (N5) and one carboxylate
oxygen atom (O4A) are situated at the apical positions. The
octahedron is much distorted with the N-Cd-O angle in along the

apical position of 148.0°. Cd2 is surrounded by two carboxylate
oxygen atoms (O1 and O1B) of PA ligands and two Cl atoms
(Cl1 and Cl1B) in the equatorial plane as well as two nitrogen
atoms (N4A and N4C) of bbi ligands at the apical positions. The
Cd-O and Cd-N bond lengths lie in range of 2.287(5)-2.334(4) Å.
Cd-Cl distance is 2.5423(14) Å. PA ligand demonstrated (κ¹)-(κ¹-
κ¹)-μ₃ coordination mode, bridging two Cd1 and one Cd2 with
Cd1B...Cd1C and Cd2...Cd1C (symmetry codes: B, 1-x, 1-y, 1-z;
C, 0.5-x, -0.5+y, 0.5-z.) distances across the naphthyl ring of
12.91(8) and 14.06(5) Å, respectively. The dihedral angle of two
naphthyl ring is 84.1°. Both bbi ligands adopt *GGG* conformation
but different dihedral angles between two imidazole rings (112.8 °
for bbi1 and 0 ° for bbi2). Through the bridging of two *syn-syn*
carboxylate groups and two μ²-bridged Cl atoms, a novel linear
trinuclear [Cd₃(μ²-CO₂)₂(μ²-Cl)₂] core is formed. Cd2 is located
at the vertex and doubly bridged to adjacent Cd1 ions. Cd1 and
Cd2 are separated with the distance of 4.1457(5) Å. The Cd-Cl-
Cd angle is 102.6(4)°. These trinuclear cores are bridged through
PA and bbi1 ligands along the *ac* plane to generate 2-D layers
(Figure 5b). Bbi2 ligands as pillars, link the layers further to form
3D framework (Figure 5c). In such a way, each Cd₃ core is linked
to other six cores through four PA ligands and four bbi ligands.
Topologically, if each Cd₃ core was considered as an irregular
six-connected node and the whole framework could be
represented as an α-Po topology with the Schläfli symbol of 4¹²6³
(Figure 5d and 5e). In this definition, one PA ligand and bbi1
connecting two adjacent Cd₃ cores were viewed as one linear
linker.

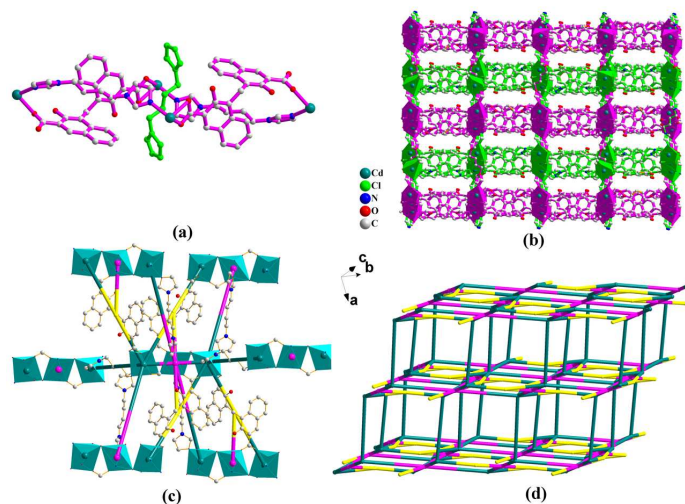


Figure 6. (a) and (b) View of polyrotaxane motif and 2-fold interpenetration. (c) The connectivity of Cd center with the ligands. (d) Topological representation of (3,5,6)-connected net.

Further investigation on the structure of compound **5** indicated
that the fascinating structure also possesses both polyrotaxane
and polycatenane. The connectivity of two Cd2 atoms, two PA
ligands and two bbi ligands (bbi2) form a large loop. Two nets
interlock with each other with the loops of each net penetrated by
bbi ligand (bbi1) of the other and vice versa (Figure 6a and 6b).
Consequently, the topology of the net could be better described if
each Cd center was viewed as nodes. The PA ligand in (κ¹)-(κ¹-
κ¹)-μ₃ coordination mode bridges three Cd ions and may be
considered as a distorted planar 3-connected node. Cd1 and Cd2

are 5- and 6-connected, respectively. The whole framework is represented as trinodal (3,5,6)-connected topology with the Schläfli symbol of $(3.5.6)_{PA}(3.5^2.6^7)_{Cd1}(3^2.5^4.6^6.7^2.9)_{Cd2}$ (Figure 6c and 6d).

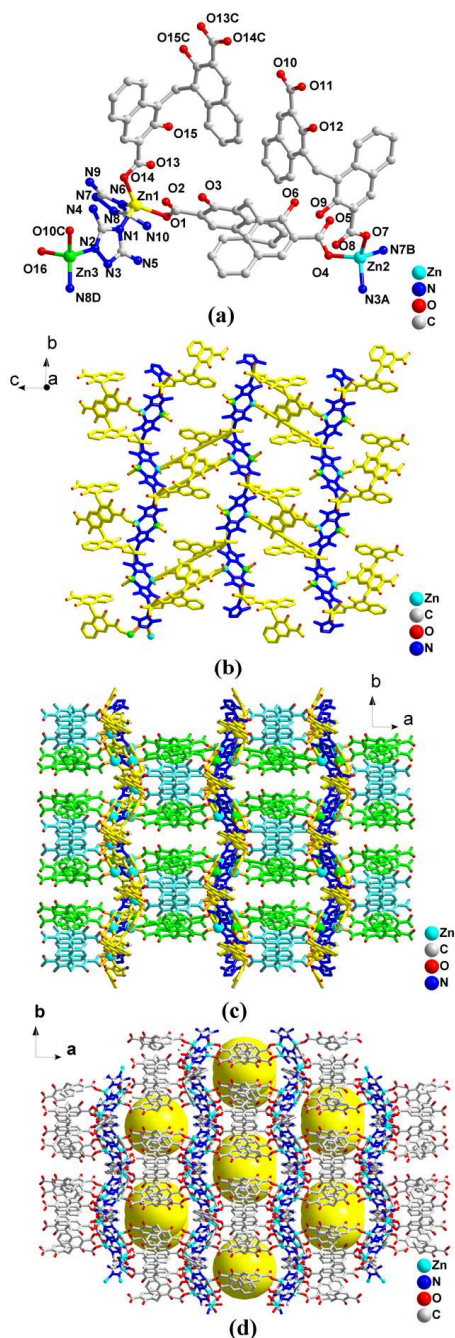


Figure 7. (a) The coordination environment around Zn centers in 6. Symmetry code: A, $1/2-x, 1/2-y, -z$; B, $x, 1-y, -1/2+z$; C, $1-x, y, 1/2-z$; D, $1/2-x, -1/2+y, -1/2-z$. (b) Perspective View of the 2-D sheet along the bc plane, showing the connectivity between the Zn-datrz based chains and PA ligands. (c) View of 3-D framework of 6 along ab plane. For clarity, three crystallographically independent PA ligands are represented by yellow, blue and skyblue bonds, respectively. (d) View of the pores within the 3-D framework.

Compound 6 crystallizes in the space group $C2/c$ and in the crystal system of Monoclinic. The asymmetric unit consists of three crystallographically independent Zn atoms, two and a half PA ligands (O1-O6, PA1; O7-O12, PA2; O13-O15, PA3), one datrz⁻ anion ligand (N1-N5) and one amine-protonated Hdatz ligand (N6-N10) as well as one coordinated aqua molecule (Figure 7a). All the Zn(II) ions adopt four-coordinated tetrahedral geometry, while the coordination atoms are different. Zn1 is coordinated with two monodentate carboxylate oxygen atoms (O1 and O14) from different PA ligands and two μ -1-N atoms (N1 and N6) of datrz⁻ anion and Hdatz ligands. Zn2, however, is bonded to two monodentate carboxylate oxygen atoms (O4 and O7) from different PA ligands and two μ -3-N atoms (N3A and N7B) of datrz⁻ anion and Hdatz ligands. Four coordination atoms around Zn3 come from one monodentate carboxylate oxygen atom (O10C) of PA ligand, two μ -4-N atoms (N2 and N8D) of datrz⁻ anion ligands and one coordinated aqua oxygen atom (O16). The Zn-O and Zn-N bond lengths lie in range of 1.939(5)-2.028(4) Å. Three independent PA ligands all exhibit $(\kappa^1-\kappa^0)-(\kappa^1-\kappa^0)-\mu_2$ coordination modes and the dihedral angles of naphthyl rings in each ligand are 88.5, 95.9 and 84.4°, respectively.

Zn2 and Zn3 are connected by datrz⁻ anion and Hdatz ligand through μ -3,4-bridging mode to form a dimeric unit, $[Zn_2N_4O_4]$, with the $Zn2 \cdots Zn3$ separation of 3.64(2) Å. These units are linked to Zn1 atoms through a triazole unit, generating a 1-D zigzag banded structure (Figure 7b). Each band is bonded with other eight bands through PA ligands in different conformations, forming an overall 3-D network (Figure 7c). Through the special connectivity of the ligands with Zn atoms, pores were generated within the network (Figure 7d and Figure S3 in Supporting Information). The potentially accessible solvent volumes are 11991.8 \AA^3 , 56.0% in per unit as calculated by PLATON.

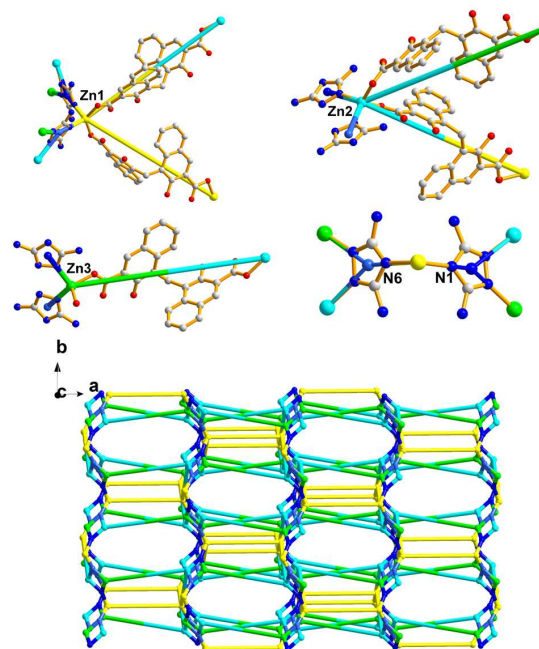


Figure 8. Topological representation of the (3,3,3,4,4)-connected network of 6.

Topologically, each datrz^- anion or Hdatrz ligand bridges three Zn centers and acts as a planar 3-connected node, respectively. Zn1 and Zn2, in turn, are surrounded by two PA and two datrz^- ligands, which can be viewed as distorted tetrahedral 4-connected nodes. Due to the coordination of aqua molecule, however, Zn3 was viewed as planar 3-connected nodes connected with one PA and two datrz^- ligands. Consequently, the whole net is constructed by pentanodal (3,4)-connected nodes with the point symbol of $(4.5.6)_{\text{datrz}1}(4.8.10)_{\text{datrz}2}(5^2.6.8.9.11)_{\text{Zn}1}(4.5.6.8.9^2)_{\text{Zn}2}(4.5.7)_{\text{Zn}3}$. The current framework represents, as far as we know, an unprecedented case of such mixed nodes (Figure 8).

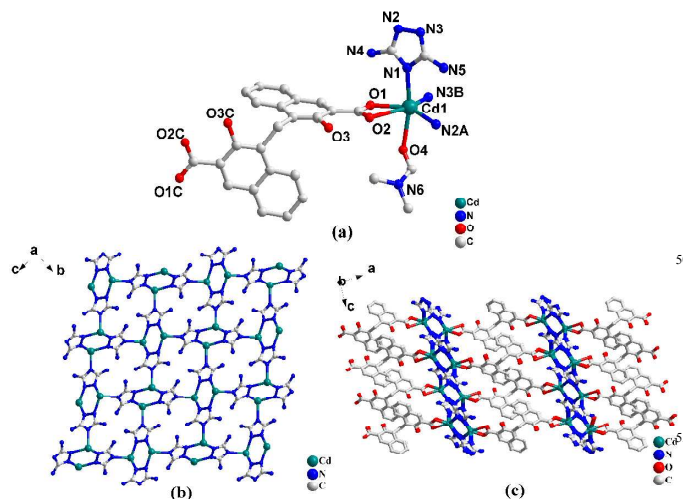
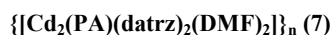


Figure 9. (a) The coordination environment around Cd centers in 7. Symmetry code: A, $x, 2-y, 1/2+z$; B, $1/2-x, -1/2+y, 1/2-z$; C, $-x, y, 1/2-z$. (b) and (c) Perspective and topological view of the 2-D Cd-datrz sheet along the bc plane, showing the connectivity between the Cd(II) ions and the triazole ligands. (d) and (e) Perspective and topological view of 3D framework of 7.

Compound 7 crystallizes in the crystal system of monoclinic and space group $C2/c$. The asymmetric unit consists of one Cd(II) ions, half PA ligand, one datrz^- anion ligand as well as one coordinated DMF molecule (Figure 9a). Cd1 adopts six-connected octahedral coordination geometry. Two chelating oxygen atoms (O1 and O2) from PA ligand and two nitrogen atoms (N2A and N3B) from one datrz^- ligand are arranged in the equatorial plane. One nitrogen atom (N1) from datrz^- ligand and oxygen atom (O4) from DMF molecule are situated at the apical positions. The Cd–O and Cd–N bond lengths lie in range of 2.214(13)–2.805(14) Å. PA exhibits $(\kappa^1-\kappa^1)-(\kappa^1-\kappa^1)-\mu_2$ coordination mode and the dihedral angles of naphthyl rings is 84.4°, respectively.

The datrz^- ligand connected the Cd(II) ions in μ -1,2,4-bridging mode to form two-dimensional sheets along the bc plane (Figure 9b). Within the sheet, two kinds of circuits are arranged alternately, with one 6-membered ring (Cd_2N_4) and the other 16-membered ($\text{Cd}_4\text{N}_8\text{C}_4$) ring, respectively. The metal...metal distance in the former rings are 3.90(2) Å. The PA ligands act as pillars, connecting these sheets to give rise to the overall three-dimensional network (Figure 9c). The metal...metal distance

separated by PA ligand is 15.43(2) Å. Topologically, the datrz^- anions and Cd centers could be simplified to planar 3-connected and distorted tetrahedral 4-connected nodes, respectively. The whole binodal (3,4)-connected net possesses the Schafli symbol of $(4.6.8)_{\text{datrz}}(4.6^2.8^3)_{\text{Cd}}$ (Figure 10).

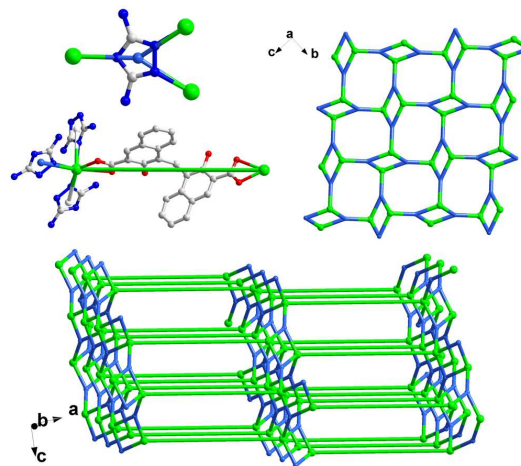
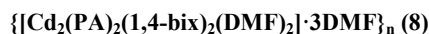


Figure 10. Topological representation of the (3,4)-connected network of 7.



Compound 8 crystallizes in the crystal system of monoclinic and space group $P2_1/c$. The asymmetric unit consists of two crystallographically independent Cd atoms, two PA ligands (O1–O6, PA-1; O7–O12, PA-2), two bix ligands (N1–N4, bix1; N5–O8, bix2) as well as two free DMF molecules (Figure 11a). Both Cd(II) ions adopt seven-connected CdO_5N_2 coordination spheres with distorted pentagonal bipyramidal geometry. The equatorial plane of Cd1 is composed of four chelating carboxylate oxygen atoms (O1, O2, O7 and O8) from two PA ligands and one nitrogen atom (N1) from bix1, while the apical positions are occupied by one nitrogen atom (N8A) of bix2 and oxygen atom (O13) of DMF molecule. For Cd2, however, two nitrogen atoms (N5 and N4C) of different bix ligands are situated at the apical positions. Four chelating carboxylate oxygen atoms (O3, O4, O10B and O11B) and one DMF oxygen atom (O14) are in the equatorial plane. The Cd–O and Cd–N bond lengths lie in range of 2.285(5)–2.599(4) Å.

Cd atoms are connected through the ligands, forming different chains along the b and c axis (Figure 11b). Firstly, Cd1 and Cd2 are alternately connected by PA1 and PA2, forming 1-D chains along the c axis with Cd...Cd separation of 15.35(2) and 14.95(2) Å. Both PA ligands present $(\kappa^1-\kappa^1)-(\kappa^1-\kappa^1)-\mu_2$ conformation, while the dihedral angles between the naphthyl rings are 78.6 and 92.1°, respectively. Secondly, bix1 and bix2 present U and Z-shaped conformation, respectively, linking Cd1 and Cd2 alternately to form helical chains along the b axis. The dihedral angles between two terminal imidazole rings in bix1 and bix2 are 78.6 and 92.1°, respectively. The repeated unit of Cd1-bix1-Cd2-bix2 is along b axis with a longer pitch of 33.0170(31) Å. Adjacent helical chains along the bc plane show opposite chirality. These chains are interconnected together to result into 3-D framework (Figure 11c and 11d). Topologically, if the Cd

centers are viewed as 4-connected nodes, the whole net exhibits a typical $SrAl_2$ topology with the Schläfli symbol of $(4^2.6^3.8)$ and the long topological vertex symbol of $4.6.6.4.6.8(2)$, respectively (Figure 12). The whole structure is composed of three such topologies interpenetrating with each other.

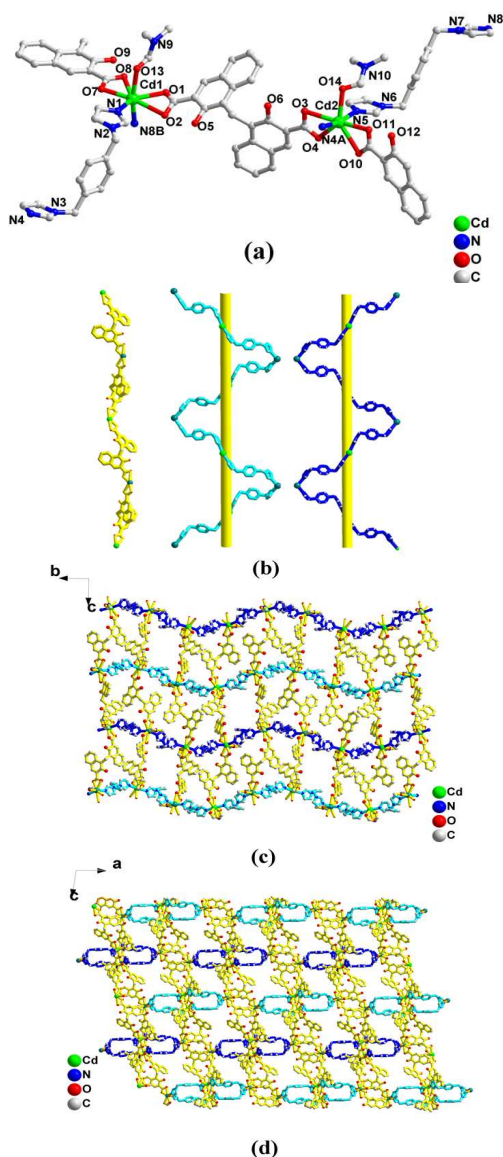


Figure 11. (a) The coordination environment around Cd center in 8. Symmetry codes: A, $-x, 1-y, 1-z$; B, $-2+x, 0.5-y, -0.5+z$. (b) View of three different chain motifs, showing the right- and left-handed helices through Cd and bix ligands. (c) and (d) Perspective view of the 3-D framework along a and b axis, respectively.

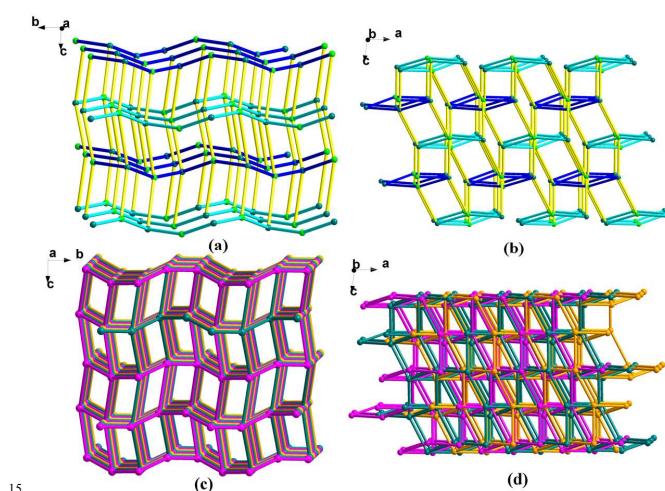


Figure 12. (a) and (b) Topological view of the 3-D framework along a and b axis, respectively. (c) and (d) Topological view of the 3-fold interpenetration along a and b axis, respectively.

20 Mixed-ligand Effect of the structures.

As many other multicarboxylate acid ligands, H_2PA is a semi-rigid ligand containing both conjugated naphthyl rings and flexible $-CH_2-$ group. It can adopt different conformations via bending, stretching, or twisting. The coordination modes and a superimposed picture of PA ligand in eight compounds was put this into perspective (Figure 13). Meanwhile, the basic N-donor ligands could also cooperate with PA by adjusting their conformations to generate coordination diversity of the metal centers, the geometry of the metal nodes and further the assembly of the whole networks. As far as we know, about thirty mixed-ligand coordination compounds have been reported based on PA ligands with different N-containing ligands, such as pyridine, 2,2-bipyridine, phen, 4,4'-bipyridine, bpe, bpea, bpp, bbi and bix and so on.^{14, 16-24} Herein, only 4,4'-bipyridine, bpe, bpea, bpp, datrz and bix were considered for discussion.^{14, 16-22} The structural characteristics of these compounds including our work in this manuscript were listed in Table 2, referring to the whole network, detailed connectivity of PA and N-containing ligands.

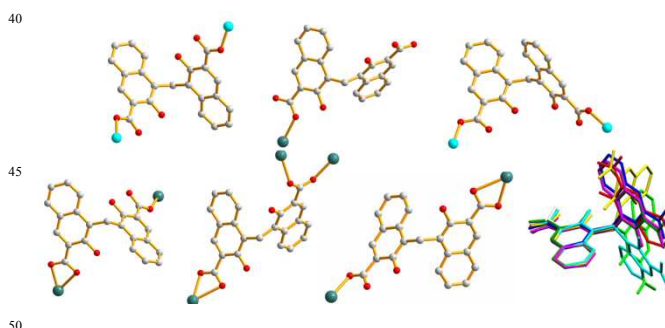


Figure 13. Coordination modes and a superimposed picture of PA ligand (bottom, right) in compounds 1-8.

In all compounds, the PA ligand connects different metal atoms into substructures including 0-D molecule, loop, 1-D linear/zigzag chains, 2-D layer and 3-D complicated architectures. Its conformational variations can broadly be quantified by two

important parameters: coordination modes and dihedral angles of two naphthyl rings. The ligands exhibited six kinds of coordination modes in all compounds depending on the coordinated metal centers. For smaller metal atoms, including Ni, Cu and Zn, simple bis(monodentate) mode is observed. For larger metal atoms, such as Cd, the two carboxylate groups adopt bisdentate chelating or tetradentate modes. Generally, the dihedral angles of two naphthyl rings are in the range 77.8 to 102.7° with a few examples being 109 and 136.7°, respectively. Most of these angles are smaller than that of the free pamoic acid (95.6°).

N-containing ligands, however, bridge metal atoms to form 1-D zigzag chains, 1-D helical chains, 1-D bands, 2-D layers as well as 3-D structures. The different connectivity is largely dependent on the N-ligands themselves, especially the rigidity and flexibility. Almost all the coordination polymers based on 4,4'-bipy possess 2-D (4,4) grid layer, while those with most flexible ligands, including bpea, bpp, bbi and bix, exhibit various and more complicated architectures. Of course, the aspects of spacer effect, positional isomeric effect, and substituent effect of the organic building blocks also have influence on the resulting structures. It is notable that the large metal-metal separation of 12-15Å by these ligands of course easily cause the penetration and tend to flexibly constitute more compact lattice architectures.

Powder XRD diffractions and Thermogravimetric analysis.

Powder XRD diffractions of compounds **1-8** were shown in Figure S5 in the Supporting Information. All the peaks measured were similar to those in the simulated patterns, indicating the purity of all the compounds. Thermogravimetric analysis (TG) was performed on compounds **1-8** to investigate their thermal stability (Figure S6 in the Supporting Information). The TG curves of compounds **1**, **3**, **4** and **5** are similar. No weight loss was observed before 340 °C. From then on the rapid weight loss occurred, suggesting the decomposition of the whole structures. For compound **2**, the weight loss from 40 to 100 °C corresponds to the free aqua molecules (calcd 2.59%, obsd 3.05%). The weight remains unchanged until about 320 °C. The TG curve of compound **6** displays steady weight loss from room temperature to 220 °C (obsd 29.97%), corresponding to the loss of the free DMF molecules (calcd 29.80%), which is followed by the framework collapse with increasing temperature. Compound **7** releases the terminal DMF molecules in the temperature range of 185 to 245 °C (calcd 84.69%, obsd 84.75%). This compound starts to decompose above 360 °C. For compound **8**, the loss of the lattice and coordinated DMF molecules (calcd 22.09%) occurs in 120-260 °C (obsd 23.79%) and the rapid weight loss in the temperature range 310-410 °C indicates the decomposition of the structure. Moreover, PXRD analyses indicate compounds **6** and **8** are also insoluble and stable in organic solvents, including DMF, MeOH, EtOH and CH₃CN (Figure S7 in the Supporting Information).

Fluorescent properties.

Coordination compounds with d¹⁰ metal centers, have generally been investigated for fluorescence properties. The solid photoluminescence spectra of compounds **1-8** were measured in the solid state at room temperature (Figure 14). Datz ligand is

nearly nonfluorescent in the range 400-800 nm for excitation wavelengths between 250 and 450 nm.²⁵ Free PA ligand, bpp, bbi and bix ligand shows an emission at 474 nm ($\lambda_{\text{ex}} = 430$ nm), 446 nm ($\lambda_{\text{ex}} = 348$ nm), 420 nm ($\lambda_{\text{ex}} = 340$ nm), 392 nm ($\lambda_{\text{ex}} = 340$ nm), respectively (Figure S8 in the Supporting Information). These emissions may be ascribed to the intraligand $\pi \rightarrow \pi^*$ or $\pi^* \rightarrow n$ transitions.^{21, 26} Comparably, eight compounds display a wide range of emission behaviors with the respective maximum at 635 nm with the shoulder peak at 525 nm ($\lambda_{\text{ex}} = 362$ nm) for **1**, 589 nm ($\lambda_{\text{ex}} = 363$ nm) for **2**, 634 and 504 nm ($\lambda_{\text{ex}} = 362$ nm) for **3**, 635 nm ($\lambda_{\text{ex}} = 367$ nm) for **4**, 569 nm ($\lambda_{\text{ex}} = 360$ nm) for **5**, and 581 nm ($\lambda_{\text{ex}} = 363$ nm) for **6**, 599 nm ($\lambda_{\text{ex}} = 364$ nm) for **7**, 531 nm with the shoulder peak at 502 nm ($\lambda_{\text{ex}} = 362$ nm) for **8**, respectively.

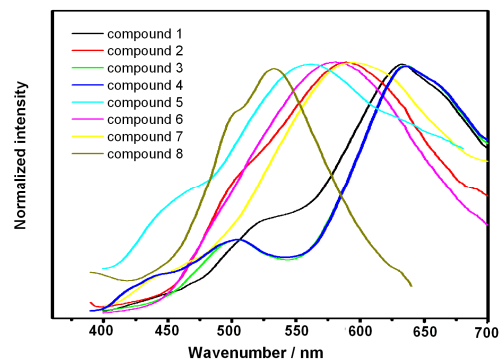


Figure 14. The solid state fluorescent spectra of compounds **1-8** at room temperature.

According to the references, Zn(II) and Cd(II) ions are difficult to oxidize or to reduce. As a result, the emission bands should be ascribed to neither MLCT (metal-to-ligand charge transfer) nor LMCT (ligand-to-metal charge transfer) in nature, but the intraligand transitions. The luminescence may be attributed to the ligation of the ligand to the metal center with different coordination modes and conformations. The coordination enhances the "rigidity" of the ligand and thus reduces the loss of energy through a radiationless pathway.²⁷ Additionally, as previously reported for mixed-ligand system, fluorescent emission of carboxylate ligands resulting from the $\pi^* \rightarrow n$ transition is very weak compared with that of the $\pi^* \rightarrow \pi$ transition of the N-donor ligands, so solid-state carboxylate ligands almost have no significant contribution to the as-synthesized coordination polymers. Therefore, the emission bands would be assigned to $\pi^* \rightarrow \pi$ transition of corresponding bis(pyridyl) ancillary ligands.²⁸ Moreover, related calculations have suggested that the luminescence band gaps between the highest occupied molecular orbitals (HOMOs) and the lower unoccupied molecular orbitals (LOMOs) can be altered by changing the degree of conjugation in the ligand and also be influenced by the degree of interligand coupling.²⁹ As a result, the weak interactions, especially $\pi \cdots \pi$ stacking interactions in the crystalline lattice, may also affect the rigidity of the whole network and further the energy transfer involved in the luminescence.

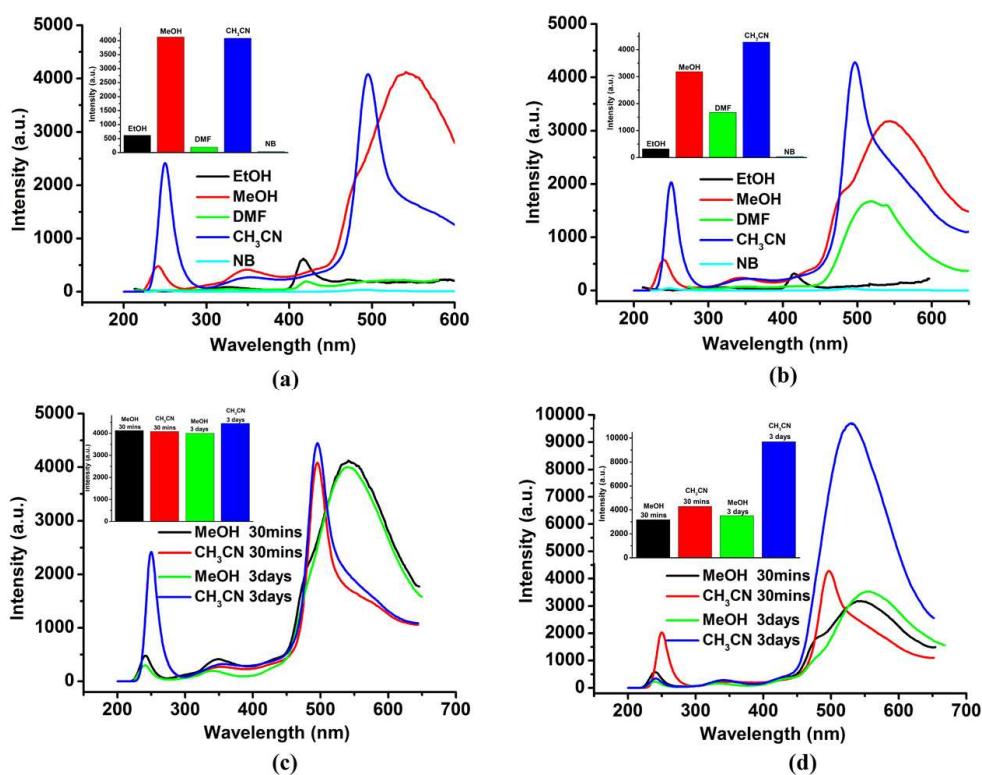


Figure 15. (a) and (b) Emission spectra of compounds **6** and **8** in different solvents. (c) and (d) Emission spectra of compounds **6** and **8** after immersing in MeOH and CH₃CN for 30 minutes and 3 days, respectively.

5 Fluorescent properties of compounds **6** and **8** in diverse solvent suspensions were also investigated. The suspensions were prepared by introducing 2 mg of finely ground sample of the ligand and compounds into 4mL solvents, including methanol (MeOH), ethanol (EtOH), acetonitrile (CH₃CN), N,N'-dimethylformate (DMF) and nitrobenzene (NB), respectively. Before measurements, the suspension was treated with ultrasonication for 30 minutes. As shown in Figure 15a and 15b, the luminescence intensities of these two compounds are largely dependent upon the solvent molecules. This phenomenon may be attributed to the interactions of the solvents with some sites of the compounds, which can influence the energy transfer process.³⁰ Additionally, to investigate the effect of the contacting time on the suspensions, the suspensions of compounds **6** and **8** in MeOH and CH₃CN were measured after 3 days. The intensities of compound **6** remains almost unchanged in these solvents while the intensities of compound **8** in CH₃CN increases greatly (Figure 15c and 15d), which may suggest the stronger energy transfer process in this system.

It is notable that the emission bands for most solvents used were visible, while for NB the luminescence signals completely disappeared. That is, the luminescent intensity shows a remarkable quenching effect. So far, CPs showing luminescent sensing properties for nitro-aromatic compounds have been reported.³¹⁻³³ The quenching phenomena may be ascribed to the energy transfer from the electron-donating frameworks of these CPs to the highly electron-withdrawing nitro group of NB. When NB was added to the suspensions of compounds **6** and **8** in MeOH, the peaks intensity around 552 and 548 nm was reduced with increasing concentration of NB (Figure S9 in Supporting

Information). The quenching effect can also be quantitatively determined by the Stern-Volmer equation: $I_0/I = 1 + K_{sv}[Q]$, where the I_0 and I are the fluorescence intensities of fluorophore in the absence and presence of compounds, respectively. $[Q]$ is the concentration of quencher and K_{sv} is the Stern-Volmer quenching constant. The inset plot of I_0/I versus $[Q]$ exhibits a good linear relationship. The K_{sv} value for these two compounds is calculated to be 1.63×10^3 and 1.09×10^4 M⁻¹, respectively, suggesting stronger quenching effect of the latter compound system. This specific quenching effect may indicate that these two compounds could serve as potential luminescent sensors in detecting traces of NB.

Conclusion.

Eight coordination compounds have been synthesized through the reaction of zinc and cadmium salts with pamoic acid (H₂PA) and different N-donor ligands. The assembly of these ligands in different coordination modes and conformations lead to fascinating structures and properties. The results demonstrate that H₂PA and these N-donor ligands are excellent candidates for the construction of CPs through so-called mixed-ligand synthetic strategy. Fluorescent properties of all compounds in solid state indicate that these compounds may be potential fluorescence materials. The luminescent properties of compounds **6** and **8** in different solvent suspensions show these two compounds could be potentially used as a fluorescence sensor for nitrobenzene in solution through significant fluorescence quenching.

Acknowledgement.

We are thankful to the National Natural Science Foundation of

China (No. 20801025), the Natural Science Foundation of Shandong Province (No. ZR2012BQ023), and the University Scientific Research Development Plan of the Education Department of Shandong Province (No. J14LC10).

References

- 1 (a) M. Li, D. Li, M. O. Keeffe and O. M. Yaghi, *Chem. Rev.*, 2014, **114**, 1343; (b) J. A. Mason, M. Veenstra and J. R. Long, *Chem. Sci.*, 2014, **5**, 32; (c) M. Zhao, S. Ou and C. D. Wu, *Acc. Chem. Res.*, 2014, **47**, 1199; (d) T. R. Cook, Y. R. Zheng and P. J. Stang, *Chem. Rev.*, 2013, **113**, 734; (e) W. M. Xuan, C. F. Zhu, Y. Liu and Y. Cui, *Chem. Soc. Rev.*, 2012, **41**, 1677; (f) D. Zhao, D. J. Timmons, D. Q. Yuan and H. C. Zhou, *Acc. Chem. Res.*, 2011, **44**, 123.
- 2 (a) H. L. Jiang, D. W. Feng, K. C. Wang, Z. Y. Gu, Z. W. Wei, Y. P. Chen and H. C. Zhou, *J. Am. Chem. Soc.*, 2013, **135**, 13934; (b) X. Q. Zhou, H. Ren and G. S. Zhu, *Chem. Commun.*, 2013, **49**, 3925; (c) S. S. Iremonger, R. Vaidhyanathan, R. K. Mah and G. K. H. Shimizu, *Inorg. Chem.*, 2013, **52**, 4124; (d) H. Q. Ma, D. Sun, L. L. Zhang, R. M. Wang, V. A. Blatov, J. Guo and D. F. Sun *Inorg. Chem.*, 2013, **52**, 10732; (e) X. K. Song, M. Oh and M. S. Lah, *Inorg. Chem.*, 2013, **52**, 10869; (f) Y. B. He, W. Zhou, R. Krishna and B. L. Chen, *Chem. Commun.*, 2012, **48**, 11813.
- 3 (a) B. Li, H. L. Wang and B. L. Chen, *Chem. Asian. J.*, 2014, **9**, 1474; (b) X. Q. Huang, Y. F. Chen, Z. G. Lin, X. Q. Ren, Y. Song, Z. Z. Xu, X. M. Dong, X. G. Li, C. W. Hu and B. Wang, *Chem. Commun.*, 2014, **50**, 2624; (c) R. Li, X. Q. Ren, J. S. Zhao, X. Feng, X. Jiang, X. X. Fan, Z. G. Lin, X. G. Li, C. W. Hu and B. Wang, *J. Mater. Chem. A.*, 2014, **2**, 2168; (d) L. Li, S. L. Xiang, S. Q. Cao, J. Y. Zhang, G. F. Ouyang, L. P. Chen and C. Y. Su, *Nature. Chem.*, 2013, **4**, 1774; (e) Z. J. Zhang, Y. G. Zhao, Q. H. Gong, Z. Li and J. Li, *Chem. Commun.*, 2013, **49**, 653; (f) Z. J. Lin, Y. B. Huang, T. F. Liu, X. Y. Li and R. Cao, *Inorg. Chem.*, 2013, **52**, 3127; (g) M. G. Goesten, F. Kapteijn and J. Gascon, *CrystEngComm.*, 2013, **15**, 9249.
- 4 (a) Z. W. Wei, W. G. Lu, H. H. Jiang and H. C. Zhou, *Inorg. Chem.*, 2013, **52**, 1164; (b) Y. W. Li, J. R. Li, L. F. Wang, B. Y. Zhou, Q. Chen and X. H. Bu, *J. Mater. Chem. A.*, 2013, **1**, 495; (c) X. Feng, L. F. Ma, L. Lang, L. Y. Wang, H. L. Song and S. Y. Xie, *Cryst. Growth. Des.*, 2013, **13**, 4469; (d) B. Liu, D. S. Li, L. Hou, G. P. Yang, Y. Y. Wang and Q. Z. Shi, *Dalton. Trans.*, 2013, **42**, 9822; (e) K. Konstas, T. Osl, Y. X. Yang, M. Batten, N. Burke, A. J. Hill and M. R. Hill, *J. Mater. Chem.*, 2012, **22**, 16698; (f) W. M. Xuan, M. N. Zhang, Y. Liu, Z. J. Chen and Y. Cui, *J. Am. Chem. Soc.*, 2012, **134**, 6904; (g) C. Hou, Q. Liu, J. Fan, Y. Zhao, P. Wang and W. Y. Sun, *Inorg. Chem.*, 2012, **51**, 8402; (h) J. S. Hu, L. Qin, M. D. Zhang, X. Q. Yao, Y. Z. Li, Z. J. Guo, H. G. Zheng and Z. L. Xue, *Chem. Commun.*, 2012, **48**, 681.
- 5 (a) A. M. Bohnsack, I. A. Ibarra, V. I. Bakhmutov, V. M. Lynch and S. M. Humphrey, *J. Am. Chem. Soc.*, 2013, **135**, 16038; (b) S. N. Wang, S. S. Xiong, Z. Y. Wang and J. F. Du, *Chem. Eur. J.*, 2011, **17**, 8630; (c) O. K. Farha and J. T. Hupp, *Acc. Chem. Res.*, 2010, **43**, 1166; (d) O. K. Farha, C. D. Malliakas, M. G. Kanatzidis, M. G. Kanatzidis and J. T. Hupp, *J. Am. Chem. Soc.*, 2010, **132**, 950.
- 6 (a) M. Xue, G. S. Zhu, Y. J. Zhang, Q. R. Fang, I. J. Hewitt and S. L. Qiu, *Cryst. Growth. Des.*, 2008, **8**, 427; (b) M. Du, Z. H. Zhang, L. F. Tang, X. G. Wang, X. J. Zhao and S. R. Batten, *Chem. Eur. J.*, 2007, **13**, 2578; (c) M. O'Keffe, M. A. Peskov, S. J. Ramsden and O. M. Yaghi, *Acc. Chem. Res.*, 2008, **41**, 1782; (d) L. Han and M. C. Hong, *Inorg. Chem. Commun.*, 2005, **8**, 406; (e) B. Kesanli and W. B. Lin, *Coord. Chem. Rev.*, 2003, **246**, 305.
- 7 (a) M. Du, C. P. Li, C. S. Liu and S. M. Fang, *Coord. Chem. Rev.*, 2013, **257**, 1282 and references therein; (b) H. Wang, W. T. Yang and Z. M. Sun, *Chem. Asian. J.*, 2013, **8**, 982; (c) Y. J. Ban, Y. S. Li, X. L. Liu, Y. Peng and W. S. Yang, *Micropor. Mesopor. Mat.*, 2013, **173**, 29.
- 8 (a) G. A. Senchyk, A. B. Lysenko, H. Krautscheid, E. B. Rusanov, A. N. Chernega, K. W. Kramer, S. X. Liu, S. Decurtins and K. V. Domasevitch, *Inorg. Chem.*, 2013, **52**, 863; (b) C. L. Jiao, F. Li, J. Zhang, Z. P. Li, S. Wang, Z. G. Wang, H. Yu, Z. B. Li, S. Liu and Z. Q. Wang, *Dalton. Trans.*, 2013, **42**, 1346; (c) D. Sun, S. Yuan, H. Wang, H. F. Lu, S. Y. Feng, D. F. Sun, *Chem Commun.*, 2013, **49**, 6152; (d) D. Sun, Z. H. Yan, V. A. Blatov, L. Wang, D. F. Sun, *Cryst Growth Des.*, 2013, **13**, 1277.
- 9 (a) X. T. Zhang, L. M. Fan, X. Zhao, D. Sun, D. C. Li and J. M. Dou, *CrystEngComm.*, 2012, **14**, 2053; (b) G. Y. Jiang, T. Wu, S. T. Zheng, X. Zhao, Q. P. Lin, X. H. Bu and P. Y. Feng, *Cryst. Growth. Des.*, 2011, **11**, 3713; (c) D. Sun, Q. J. Xu, C. Y. Ma, N. Zhang, R. B. Huang, L. S. Zheng, *CrystEngComm*, 2010, **12**, 4161; (d) M. Du, X. J. Jiang and X. J. Zhao, *Inorg. Chem.*, 2007, **46**, 3984.
- 10 (a) S. Wang, R. Yun, Y. Peng, Q. Zhang, J. Lu, J. Dou, J. Bai, D. Li and D. Q. Wang, *Cryst. Growth. Des.*, 2012, **12**, 79; (b) T. Y. Min, B. Zheng, J. F. Bai, R. Sun, Y. Z. Li and Z. X. Zhang, *CrystEngComm.*, 2010, **12**, 70; (c) S. N. Wang, H. Xing, Y. Z. Li, J. F. Bai, M. Scheer, Y. Pan and X. Z. You, *Chem. Commun.*, 2007, 2293; (d) S. N. Wang, J. F. Bai, Y. Z. Li, Y. Pan, M. Scheer and X. Z. You, *CrystEngComm.*, 2007, 1084; (e) S. N. Wang, H. Xing, Y. Z. Li, J. F. Bai, Y. Pan, M. Scheer and X. Z. You, *Eur. J. Inorg. Chem.* 2006, 3041.
- 11 (a) B. F. Hoskins, R. Robson and D. A. Slizys, *J. Am. Chem. Soc.*, 1997, **119**, 2952; (b) L. Ballester, I. Baxter, P. C. M. Duncan, D. M. L. Goodgame, D. A. Grachvogel and D. J. Williams, *Polyhedron*, 1998, **17**, 3613.
- 12 (a) Sheldrick, G. M. SHELXS-97, Program for Crystal Structure Solution; Göttingen University: Göttingen, Germany, 1997. (b) Sheldrick, G. M. SHELXL-97, Program for Crystal Structure Refinement; Göttingen University: Göttingen, Germany, 1997.
- 13 Spek, A. L. *J. Appl. Cryst.* 2003, **36**, 7.
- 14 S. N. Wang, Y. Q. Peng, X. L. Wei, Q. F. Zhang, D. Q. Wang, J. M. Dou, D. C. Li and J. F. Bai, *CrystEngComm.*, 2011, **13**, 5313.
- 15 X. L. Wang, C. Qin, E. B. Wang and L. Xu, *Cryst. Growth. Des.* 2006, **6**, 2061.
- 16 F. Luo, Y. T. Yang, Y. X. Che and J. M. Zheng, *CrystEngComm.*, 2008, **10**, 981.
- 17 X. M. Shi, M. X. Li, X. He, H. J. Liu and M. Shao, *Polyhedron*, 2010, **29**, 2075.
- 18 L. N. Zhang, X. L. Sun, C. X. Du and H. W. Hou, *Polyhedron*, 2014, **72**, 90.
- 19 M. Du, C. P. Li, X. J. Zhao and Q. Yu, *CrystEngComm.*, 2007,

- 9, 1011.
- 20 C. W. Lv, J. Li, Z. Hou and M. K. Li, *J. Inorg. Organomet. P.*, 2014, **24**, 388.
- 21 J. J. Wang, M. L. Yang, H. M. Hu, G. L. Xue, D. S. Li and Q. Z. Shi, *Inorg. Chem. Comm.*, 2007, **10**, 269.
- 22 Y. Q. Peng, X. L. Wei, D. C. Li and S. N. Wang, *Acta Cryst. E.*, 2012, **68**, m125.
- 23 Z. X. Han, J. J. Wang, H. M. Hu, X. L. Chen, Q. R. Wu, D. S. Li and Q. Z. Shi, *J. Mol. Struct.*, 2008, **891**, 364.
- 24 Q. Shi, Y. T. Sun, L. Z. Sheng, K. F. Ma, M. L. Hu, X. G. Hu and S. M. Huang, *Cryst. Growth. Des.*, 2008, **8**, 3401.
- 25 A. K. Paul, U. Sanyal and S. Natarajan, *Cryst. Growth. Des.*, 2010, **10**, 4161.
- 26 (a) Z. H. Li, L. P. Xue, S. H. Li, J. G. Wang, B. T. Zhao, J. Kan and W. P. Su, *CrystEngComm.*, 2013, **15**, 2745; (b) X. Li, X. Guo, X. Weng and S. Lin, *CrystEngComm.*, 2012, **14**, 1412.
- 27 (a) J. Guo, J. F. Ma, B. Liu, W. Q. Kan and J. Yang, *Cryst. Growth Des.*, 2011, **11**, 3609; (b) X. L. Yang, M. H. Xie, C. Zou and C. D. Wu, *CrystEngComm.*, 2010, **12**, 1779; (c) M. D. Allendorf, C. A. Bauer, R. K. Bhakta and R. J. T. Houk, *Chem. Soc. Rev.* 2009, **38**, 1330; (d) Z. Chang, A. S. Zhang, T. L. Hu and X. H. Bu, *Cryst. Growth Des.*, 2009, **9**, 4840; (e) E. Tekin, D. A. M. Egbe, J. M. Kranenburg, C. Ulbricht, S. Rathgeber, E. Birckner, N. Rehmann, K. Meerholz and U. S. Schubert, *Chem. Mater.*, 2008, **20**, 2727.
- 28 (a) W. Chen, J. Y. Wang, C. Chen, Q. Yue, H. M. Yuan, J. S. Chen and S. N. Wang, *Inorg. Chem.*, 2003, **42**, 944; (b) D. Sun, N. Zhang, R. B. Huang and L. S. Zheng, *Cryst. Growth. Des.*, 2010, **10**, 3699; (c) X. Q. Fang, Z. P. Deng, L. H. Huo, W. Wan, Z.-B. Zhu, H. Zhao and S. Gao, *Inorg. Chem.*, 2011, **50**, 12562; (d) D. Sun, Z. H. Yan, M. Liu, H. Xie, S. Yuan, H. Lu, S. Feng and D. Sun, *Cryst. Growth. Des.*, 2012, **12**, 2902; (e) Z. H. Li, L. P. Xue, S. H. Li, J. G. Wang, B. T. Zhao, J. K. and W. P. Su, *CrystEngComm.*, 2013, **15**, 2745.
- 29 (a) B. Civalieri, F. Napoli, Y. Noel, C. Roetti and R. Dovesi, *CrystEngComm.*, 2006, **8**, 364; (b) C. A. Bauer, T. V. Timofeeva, T. B. Settersten, B. D. Patterson, V. H. Liu, B. A. Simmons and M. D. Allendorf, *J. Am. Chem. Soc.*, 2007, **129**, 7136.
- 30 (a) Y. J. Cui, Y. F. Yue, G. D. Qian and B. L. Chen, *Chem. Rev.* 2012, **112**, 1126; (b) H. Wang, W. T. Wang and Z. M. Sun, *Chem. Asian J.*, 2013, **8**, 982; (c) Y. Yang, P. Du, Y. Y. Liu and J. F. Ma, *Cryst. Growth. Des.* 2013, **13**, 4781; (d) F. Y. Yi, W. Yang and Z. M. Sun, *J. Mater. Chem.* 2012, **22**, 23201.
- 31 (a) L. E. Kreno, K. Leong, O. K. Farha, M. Allendorf, R. P. Van Duyne and J. T. Hupp, *Chem. Rev.* 2012, **112**, 1105; (b) D. Tian, Y. Li, R. Y. Chen, Z. Chang, G. Y. Wang and X. H. Bu, *J. Mater. Chem. A* 2014, **2**, 1465; (c) H. M. Zhang, Y. C. He, J. Yang, Y. Y. Liu and J. F. Ma, *Cryst. Growth. Des.*, 2014, **14**, 2307; (d) D. Ma, B. Li, X. Zhou, Q. Zhou, K. Liu, G. Zeng, G. Li, Z. Li and S. Feng, *Chem. Commun.* 2013, **49**, 8964.
- 32 (a) L. B. Sun, H. Z. Xing, J. Xu, Z. Q. Liang, J. H. Yu and R. Xu, *Dalton. Trans.*, 2013, **42**, 5508; (b) H. Wang, W. T. Yang and Z. M. Su, *Chem. Asian J.*, 2013, **8**, 982; (c) N. Xu, J. Yang, Y. C. He, Y. Y. Liu and J. F. Ma, *CrystEngComm.*, 2013, **15**, 7360.
- 33 (a) Z. C. Hu, B. J. Deibert and J. Li. *Chem. Soc. Rev.*, 2014, **43**, 5815; (b) D. Banerjee, Z. C. Hu and J. Li. *Dalton. Trans.*, 2014, **43**, 10668.

Table 1. Crystal data and structure refinement information for compounds **1-8**.

Compound	1	2	3	4
formula	C ₃₆ H ₂₈ N ₂ O ₆ Zn	C ₇₂ H ₇₀ N ₄ O ₁₈ Cd	C ₃₃ H ₂₈ N ₄ O ₆ Zn	C ₃₃ H ₃₀ N ₄ O ₇ Cd
formula weight	649.97	1391.72	641.96	707.01
T (K)	298	298	298	298
Crystal system	Monoclinic	Orthorhombic	Monoclinic	Triclinic
Space group	<i>P2₁/c</i>	<i>Pbcn</i>	<i>P2₁/n</i>	<i>P-1</i>
a [Å]	11.853(6)	23.362(2)	13.1085(12)	11.0849(13)
b [Å]	12.385(6)	18.6642(16)	16.6562(16)	11.6224(14)
c [Å]	21.013(10)	14.8125(13)	13.6422(14)	13.0516(15)
α [°]	90.00	90.00	90.00	71.1410(2)
β [°]	99.597(7)	90.00	92.1850(10)	86.977(10)
γ [°]	90.00	90.00	90.00	69.7960(3)
V [Å ³]	3042(2)	6458.9(10)	2976.4(5)	1490.0(3)
Z	4	4	4	2
Dcalcd. [g cm ⁻³]	1.419	1.431	1.433	1.576
μ [mm ⁻¹]	0.858	0.416	0.878	0.790
θ range	2.39,25.07	2.584,19.754	2.864,27.787	2.462,18.361
index ranges	-14<=h<=11 -14<=k<=14 -25<=l<=24	-25<=h<=27 -16<=k<=22 -17<=l<=17	-15<=h<=15 -14<=k<=19 -16<=l<=16	-12<=h<=13 -13<=k<=11 -15<=l<=15
R ₁ , wR ₂ ^a [I> 2σ(I)]	0.0462,0.0751	0.0659,0.1852	0.0686,0.2213	0.0556,0.1031
GOF	1.063	0.847	1.023	0.838
Compound	5	6	7	8
formula	C ₇₆ H ₇₀ N ₁₂ O ₁₂ Cl ₂ Cd ₃	C ₁₇₁ H ₂₀₄ N ₃₆ O ₄₈ Zn ₆	C ₃₃ H ₃₆ N ₁₂ O ₈ Cd ₂	C ₉₅ H ₁₀₅ N ₁₅ O ₁₉ Cd ₂
formula weight	1751.54	3924.12	953.54	1985.76
T (K)	121	104	298	298
Crystal system	Monoclinic	Monoclinic	Monoclinic	Monoclinic
Space group	<i>P2₁/n</i>	<i>C2/c</i>	<i>C2/c</i>	<i>P2₁/c</i>
a [Å]	9.3381(5)	40.431(3)	36.873(3)	10.4759(11)
b [Å]	25.7913(12)	18.1158(10)	9.3152(9)	33.017(3)
c [Å]	15.3127(6)	35.3525(18)	10.9288(11)	28.548(3)
α [°]	90.00	90.00	90.00	90.00
β [°]	95.891(4)	123.886(8)	93.6430(10)	97.2880(10)
γ [°]	90.00	90.00	90.00	90.00
V [Å ³]	3668.5(3)	21496(2)	3746.2(6)	9794.6(16)
Z	2	4	4	4
Dcalcd. [g cm ⁻³]	1.586	0.851	1.691	1.148
μ [mm ⁻¹]	1.005	1.155	1.202	0.493
θ range	2.5673,28.3767	3.456,71.209	2.750,26.348	2.246,21.064
index ranges	-11<=h<=11 -30<=k<=12 -18<=l<=17	-49<=h<=49 -22<=k<=18 -40<=l<=44	-43<=h<=43 -8<=k<=11 -13<=l<=12	-12<=h<=12 -39<=k<=38 -33<=l<=25
R ₁ , wR ₂ ^a [I> 2σ(I)]	0.0597,0.1343	0.0792,0.2137	0.1043,0.3481	0.0617,0.1602
GOF	1.132	1.014	1.274	1.010

$$^a R_1 = \sum ||F_o| - |F_c|| / \sum |F_o|, wR_2 = [\sum w(\sum F_o^2 - F_c^2)^2 / \sum w(F_o^2)^2]^{1/2}$$

Table 2. Structural properties of the PA-based mixed-ligand coordination polymers containing different bidentate N-donor coligands reported in publications.

Cite this: DOI: 10.1039/c0xx00000x

www.rsc.org/xxxxxx

ARTICLE TYPE

	Compound	Structure	Coordination mode of PA and the angle of two naphthyl rings (°)	Connectivity of PA with metal atoms and M...M distance (Å)	Connectivity of N-donor ligands with metal atoms and M...M distance (Å)	
1	$\{[\text{Cd}_5(\text{OAc})_2(\text{OAc})_2(\text{OH})_2(\text{PA})_2(4,4'\text{-bipy})_2]\cdot\text{CH}_3\text{CH}_2\text{OH}\}_n$	3D coordination polymer based on pentanuclear Cd_5 units	$(\kappa^1:\kappa^1)-(\kappa^1:\kappa^1)-\mu_4$ 84.1	pentanuclear molecule Cd_5	zigzag molecule 11.77	Ref. 21
2	$[\text{Co}(\text{PA})(4,4'\text{-bipy})]_n\cdot n\text{H}_2\text{O}$	2D, (4,4) grid layer	$(\kappa^1-\kappa^1)-(\kappa^1-\kappa^1)-\mu_2$ 84.1	Zigzag chain 11.96	zigzag chain 11.24	Ref. 17
3	$[\text{Ni}(\text{PA})(4,4'\text{-bipy})(\text{H}_2\text{O})_2]_n\cdot 2n\text{CH}_3\text{CN}$	2D, (4,4) grid layer	$(\kappa^1)-(\kappa^1)-\mu_2$ 77.8	Zigzag chain 13.93	linear chain 11.26	Ref. 17
4	$\{[\text{Co}(\text{PA})(4,4'\text{-bipy})(\text{H}_2\text{O})(\text{CH}_3\text{OH})]\cdot\text{DMF}\}_n$	2D 4-connected sql layer	$(\kappa^1)-(\kappa^1)-\mu_2$ 91.7	linear chain 15.79	zigzag chain 11.47	Ref. 18
5	$\{[\text{Cd}_2(\text{PA})_2(4,4'\text{-bipy})_{1.5}(\text{H}_2\text{O})_3]\cdot 2\text{DMF}\cdot 2\text{H}_2\text{O}\}_n$	2D 3,4-connected $(6^3.6.6^2.6^2)(6^5.8)$ network	$(\kappa^2:\kappa^2)-(\kappa^2:\kappa^2)-\mu_2$ 96.8	double chain 14.98	linear chain 11.66, 11.88	Ref. 18
6	$[\text{Cu}(\text{PA})(4,4'\text{-bipy})(\text{DMF})_2]_n$	2D, (4,4) grid layer	$(\kappa^1)-(\kappa^1)-\mu_2$ 83.6	chain 15.62	chain 11.08	Ref. 19:
7	$\{[\text{Cd}(\text{PA})(4,4'\text{-bipy})_2](\text{H}_2\text{O})\}_n$	2D, (4,4) grid layer decorated with the unidentate 4,4'-bipy pendants as side arms at both sides	$(\kappa^1:\kappa^1)-(\kappa^1:\kappa^1)-\mu_2$ 86.9	chain 14.46	chain 11.77	Ref. 19
8	$\{[\text{Cd}_2(\text{PA})_2(\text{bpe})_{1.5}(\text{DMF})_2(\text{H}_2\text{O})]\cdot 2\text{DMF}\}_n$	2D→3D polythreaded motif based on (3.4)-connected $(4^2.6^3.8)(4^2.6)$ 2D sheets	$(\kappa^1:\kappa^1)-(\kappa^1:\kappa^1)-\mu_2$	Zigzag chain	molecule	Ref. 20:
9	$\{[\text{Ni}(\text{PA})(\text{bpea})(\text{H}_2\text{O})_2]\cdot\text{DMF}\}_n$	3D, 3-fold interpenetrating $(6^5.8)$ CdSO_4 net	$(\kappa^1)-(\kappa^1)-\mu_2$ 136.7	Linear chain 15.90(5)	Linear chain 13.50	Ref. 9

10	$\{\text{[Zn(PA)(bpea)]}\cdot\text{DMF}\}_n$	3D, roto-translational [2+2] interpenetrating diamondoid net	$(\kappa^1)-(\kappa^1-\kappa^1)-\mu_2$ 94.1	zigzag chain 15.10(2)	Zigzag chain 13.15	Ref. 9
11	$\{\text{[Zn(PA)(bpea)]}\cdot 2\text{DMF}\cdot\text{CH}_3\text{OH}\}_n$	3D, roto-translational [2+2] interpenetrating diamondoid net	$(\kappa^1)-(\kappa^1)-\mu_2$ 97.8	Zigzag chain 15.07(1)	Zigzag chain 13.30	Ref. 9
12	$\{\text{[Cd}_2(\text{PA})_2(\text{bpea})(\text{H}_2\text{O})]\cdot 3.5\text{H}_2\text{O}\}_n$	3D, 3-fold interpenetrating $(6^7\cdot 8)(6^4\cdot 7\cdot 8)$ net	$(\kappa^1-\kappa^1)-(\kappa^1-\kappa^1)-\mu_2$ 79.8	Linear chain 15.08	Linear chain 13.72	Ref. 9
13	$\{\text{[Ni}_2(\text{PA})_2(\text{bpp})_2(\text{H}_2\text{O})_3]\cdot 2\text{DMF}\}_n$	3D, 2-fold interpenetrating self-penetrating $(6\cdot 8^5)(6^4\cdot 8^2)$ net	$(\kappa^1)-(\kappa^1-\kappa^1)-\mu_2$ $(\kappa^1)-(\kappa^1)-\mu_2$ 86.1 and 65.1	2D layer 15.12 and 13.98	3-D 6-fold interpenetrated net 12.58 12.52	Ref. 9
14	$\{\text{[Ni(PA)(bpp)(H}_2\text{O})_2]\cdot\text{DMF}\}_n$	2D layer, 4-connected $(4^3\cdot 6^2\cdot 8)$ network	$(\kappa^1)-(\kappa^1)-\mu_2$ 109	Zigzag chain 13.94	Zigzag chain 11.78	Ref. 18:
15	$\{\text{[Cd(PA)(bpp)(CH}_3\text{OH})]\cdot\text{CH}_3\text{OH}\}_n$	3D, 4-connected $(8^3\cdot 10^2\cdot 12)$ network	$(\kappa^1:\kappa^1)-(\kappa^1:\kappa^1)-\mu_2$ 109	zigzag chain 15.12	Helical chains 11.85	Ref. 18:
16	$\{\text{[Zn(PA)(bpp)]}\}_n$	polythreading 2D \rightarrow 3D net composed of 4 ⁴ sqi undulated sheets	$(\kappa^1)-(\kappa^1)-\mu_2$ 102.7	Zigzag chain 11.85	Zigzag chain 13.61	this work
17	$\{\text{[Cd(PA)}_2(\text{Hbpp})_2(\text{H}_2\text{O})_2]\cdot 2\text{H}_2\text{O}\}_n$	0D, mononuclear molecule	$(\kappa^1)-(\kappa^1)-\mu_2$ 72.7	none		this work
18	$\{\text{[Zn(PA)(bbi)]}\}_n$	2D \rightarrow 3D polythreaded motifs composed of (4,4) sheets with helices	$(\kappa^1)-(\kappa^1)-\mu_2$ 84.8	Chain 11.55	Helical chain 9.59	this work
19	$\{\text{[Cd(PA)(bbi)(H}_2\text{O})]\}_n$	2D \rightarrow 2D interpenetrating 4-connected $(4\cdot 8^5)$ net with both polyrotaxane and polycatenane character	$(\kappa^1)-(\kappa^1-\kappa^1)-\mu_2$ 76.8	$\text{Cd}_2(\text{PA})_2$ loop 11.49	Zigzag chain 13.47 14.27	this work
20	$\{\text{[Cd}_3(\text{PA})_2(\text{bbi})_3(\text{Cl})_2]\}_n$	3D, 2-fold interpenetrating trinodal (3,5,6)-connected	$(\kappa^1)-(\kappa^1-\kappa^1)-\mu_3$ 84.1	2D layer based on Cd_3	3D 2-fold interpenetrating	this work

		(4.5.6)(5.6 ⁴ .8)(4.5.6.8.9 ²) net		units 15.910 14.049	net 13.68 13.17	
21	{[Cd ₂ (PA) ₂ (bbi)] _n }	2D, 6-connected (2 ² .4 ⁸ .6 ⁵) net with both polyrotaxane and polycatenane	(κ ¹ :κ ¹)-(κ ¹ :κ ¹)-μ ₄ 82.98	Chain based on Cd ₂ (CO ₂) ₄ unit 11.493	Linear chain 14.45	Ref. 16
22	{[Zn ₃ (PA) _{2.5} (datrz)(Hdatrz) (H ₂ O)] _n }	3D, pentanodal (3,4,4)- connected (4.5.6)(4.8.10)(5 ² .6.8.9.11)(4.5.6.8.9 ²)(4.5.7) net	(κ ¹)-(κ ¹)-μ ₂ 88.5, 95.9, 84.4	Molecule with six metal atoms and five PA ligands 14.59 14.28 15.0	Band 5.96, 5.99, 6.06, 6.07	this work
23	{[Cd ₂ (PA)(datrz) ₂ (DMF) ₂] _n }	3D, binodal (3,4)-connected (4.6.8)(4.6 ² .8 ³) net	(κ ¹ :κ ¹)-(κ ¹ :κ ¹)-μ ₂ 89.3	Singel molecule 15.43	2D layer 3.90	this work
24	{[Zn(PA)(bix)] _n }	2D, (4,4) corrugated layer	(κ ¹)-(κ ¹)-μ ₂ 102.2	Linear chain 15.51	Zigzag chain 11.35	Ref. 14
25	{[Zn(PA)(bix)]·2DMF} _n }	2D, helical (4,4) layer	(κ ¹)-(κ ¹)-μ ₂ 95.2	zigzag chain 11.14	Helical chain 11.02	Ref. 14
26	{[Zn(PA)(bix)]·3.7DMF} _n }	3D, 3-fold acentric interpenetrating diamondoid network	(κ ¹)-(κ ¹)-μ ₂ 83.0	zigzag chain 15.09	Helical chain 13.30	Ref. 14
27	{[Cd ₂ (PA) ₂ (bix) ₂ (DMF) ₂]·3DMF} _n }	3D, 2-fold interpenetrating 4-connected (4 ² .6 ³ .8) SrAl ₂ net	(κ ¹ :κ ¹)-(κ ¹ :κ ¹)-μ ₂ 78.6 92.1	Zigzag chain 15.35 14.95	Helical chain 14.13	this work
28	{[Zn(PA)(bix)]·2DMF} _n }	2D, helical (4,4) layer	(κ ¹)-(κ ¹)-μ ₂ 97.1	zigzag chain 15.27	Helical chain 10.83	Ref. 22:
29	[Cd(PA)(bix)] _n }	2D, 4-connected sql plane	(κ ¹ :κ ¹)-(κ ¹ :κ ¹)-μ ₂	chain	chain	Ref. 20